
Recycling manganese-rich electrolytic residues: a review

Fan Wang¹, Guangcheng Long^{*1}, Kunlin Ma¹, Xiaohui Zeng¹, Zhuo Tang¹, Rongzhen Dong¹, Jionghuang He¹, Minghui Shangguan¹, Qingchun Hu², Rock Keey Liew^{3,4}, Yang Li⁵, John Zhou^{*1,6}

* Guangcheng Long: longguangcheng@csu.edu.cn (Corresponding author)

* John Zhou: junliang.zhou@uts.edu.au (Corresponding author)

¹ School of Civil Engineering, Central South University, 68 South Shaoshan Road, Changsha, Hunan 410075, China

² Centre for Infrastructure Monitoring and Protection, School of Civil and Mechanical Engineering, Curtin University, Australia

³ Higher Institution Centre of Excellence (HICoE), Institute of Tropical Aquaculture and Fisheries (AKUATROP), Universiti Malaysia Terengganu, 21030 Kuala Nerus, Terengganu, Malaysia

⁴ NV Western PLT, No. 208B, Second Floor, Macalister Road, 10400 Georgetown, Penang, Malaysia

⁵ School of Resource & Environment and Safety Engineering, Hunan University of Science and Technology, Xiangtan 411021, China

⁶ Centre for Green Technology, School of Civil and Environmental Engineering, University of Technology Sydney, Sydney, NSW 2007, Australia

Abstract

Huge amounts of manganese-rich solid residues are yearly produced worldwide by industrial electrolysis, calling for advanced methods of recycling in the context of the circular economy. Here, we review manganese recycling with focus on ore reserves, electrolytic production, residue stockpiling and environmental impact, reducing the amount of residue and improving metal separation, and recycling the residues. Diposal techniques include dry disposal, wet disposal and fire roasting disposal. Residues can be recycled in buildings, functional materials and fertilizers.

Keywords: Electrolytic manganese solid residue; Source reduction; Harmless treatment; Resource utilization; Valuable; Sustainable development; Building materials; Environmental impact; Gradient utilization

Table of Content:

Abstract	1
1 Introduction	2
1.1 World manganese ore reserves and production distribution.....	3
1.2 Distribution of manganese ore reserves and production in China.....	7
1.3 Production and resource distribution of electrolytic manganese.....	9
1.4 Formation and stockpiling of Mn-rich residue.....	11
1.5 Characteristics and environmental impact of Mn-rich residue.....	14
1.6 Potential of resource utilization of Mn-rich residue as building materials.....	17
2. Mn-rich residue reduction and safe storage technology	18
2.1 Improvement of manganese ore grade.....	18

39	2.2 Leachate enhancement by Mn ²⁺	19
40	2.3 Improvement of the mineral separation degree and water content regulation.....	20
41	2.4 Limitations and future direction.....	21
42	3. Harmless pretreatments of Mn-rich residue.....	22
43	3.1 Direct dry disposal technology of Mn-rich residue.....	22
44	3.2 Wet disposal technology of Mn-rich residue.....	24
45	3.3 Fire roasting disposal of Mn-rich residue.....	26
46	3.4 Constraints and future directions for the harmless disposal of Mn-rich residue.....	27
47	4. Resource utilization of Mn-rich residue.....	27
48	4.1 Building materials resource utilization of Mn-rich residue based on chemical component regulation.....	28
49	4.1.1 Aluminosilicate phase.....	28
50	4.1.2 Resource utilization of sulfate phase in Mn-rich residue.....	29
51	4.1.3 Resource utilization on multiple-phase oxides in Mn-rich residue.....	30
52	4.2 Preparation of Mn-rich residue-based functional materials.....	32
53	4.3 Preparation of Mn-rich residue-based soil fertilizer.....	33
54	5. High-value resource utilization of Mn-rich residue.....	34
55	6. Current deficiencies and further prospects.....	38
56	7. Conclusions.....	40
57	Acknowledgements.....	42
58	Author contributions.....	42
59	References.....	42

60

61 **1 Introduction**

62 Electrolytic manganese solid residue, named ‘Mn-rich residue’, is a by-product of electrolytic
63 manganese metal production (Duan et al. 2010; He et al. 2021a; Yang et al. 2022; Wang et al. 2022a). It
64 contains harmful components such as ammonia nitrogen, soluble manganese and other heavy metals (Chen et
65 al. 2016; Wang et al. 2020; He et al. 2021b). Although numerous treatment methods have been proposed
66 recently, no sustainable and practical industrial process for treating Mn-rich residue exists. Therefore, the
67 review of the existing studies on the extraction, separation and stabilization or solidification of Mn-rich residue
68 harmful substances is imperative for an in-depth investigation. An overview of various disposal technologies
69 and a discussion of existing challenges and prospects are presented. In general, the sustainable development
70 of the electrolytic manganese industry is hampered by the complex associated minerals that limit the quality
71 of Mn-rich residue disposal. The United Nations has proposed seventeen sustainable development goals, many
72 of which focus on developing healthier and more sustainable production systems. Thus, there is an urgent need
73 to develop higher-quality disposal methods for Mn-rich residue. Aiming at this goal, the electrolytic process
74 of manganese and the formation mechanism of Mn-rich residue was first clearly described in this work. This
75 laid a foundation for clarifying the definition of Mn-rich residue and promoting the subsequent disposal of
76 Mn-rich residue.

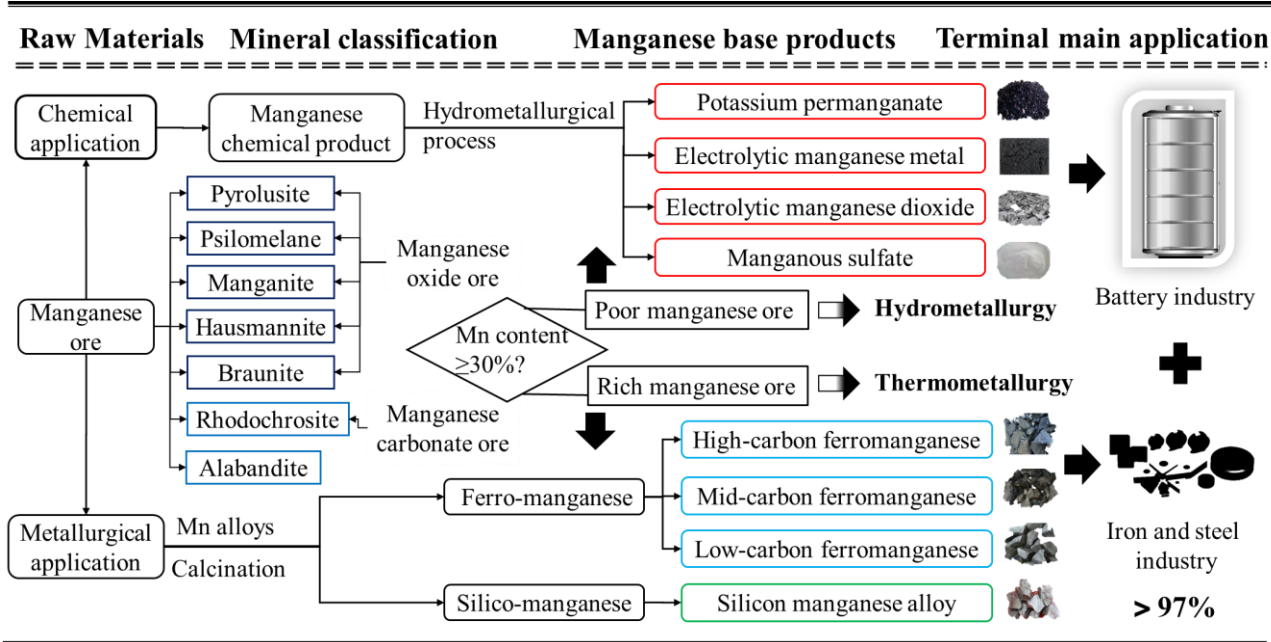
77 1.1 World manganese ore reserves and production distribution

78 The basic properties of manganese elements are essential for understanding manganese mining from the
 79 source. Manganese is a group 7 element in the fourth period of the periodic table of chemical elements. It has
 80 considerable lithophile properties in the lithosphere and silicate phase meteorites but exhibits strong
 81 oxygenophilic properties in the upper lithosphere (Liu et al. 2019). Manganese is a silver-white hard and brittle
 82 transition metal with a density of $7.44 \text{ g}\cdot\text{cm}^{-3}$, a melting point of $1244 \text{ }^\circ\text{C}$ and a boiling point of $1962 \text{ }^\circ\text{C}$.
 83 Manganese has II, III, IV, VI and VII valence states in nature, specifically +2 (Mn^{2+} compounds), +3, +4
 84 (MnO_2), +6 (manganates such as K_2MnO_4) and +7 (permanganates such as KMnO_4). The +2, +4, +6 and +7
 85 valence states of manganese exhibit high stability (Sorensen et al. 2010; Singh et al. 2020). Manganese is
 86 highly susceptible to oxidation under moist air, forming a brown laminated manganese oxide shell with an
 87 outer layer of Mn_3O_4 and an inner layer of MnO on its surface. Several common manganese minerals are
 88 described as shown in Table 1.

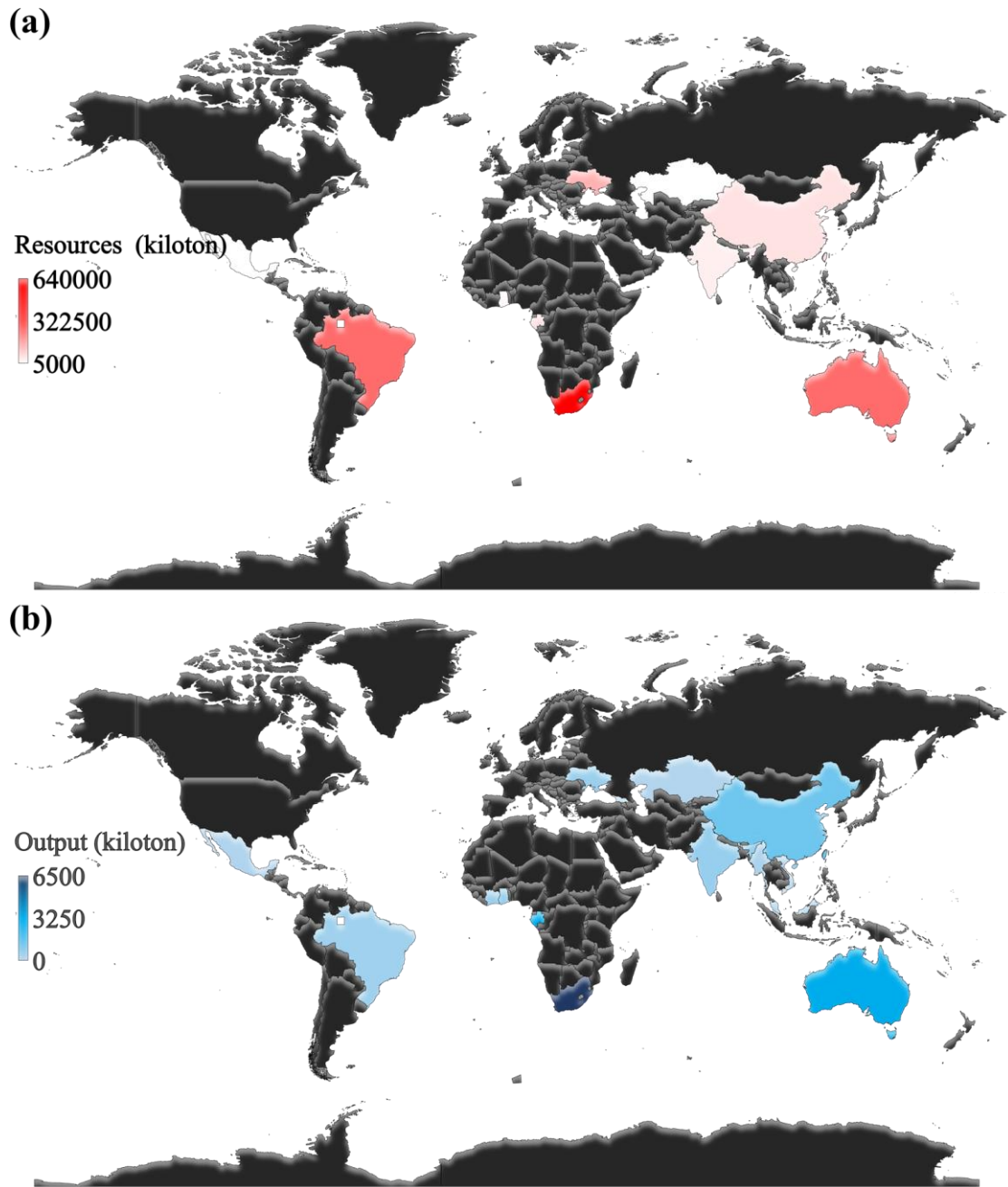
89 Table 1. The basic properties of common manganese minerals

Types	Crystals	Chemical compositions	Mn (wt.%)	Structure	Density ($\text{g}\cdot\text{cm}^{-3}$)	Rarity	Metallization
Pyrolusite	Tetragonal	MnO_2	63.2	Loose	5	Common	Sedimentation
Psilomelane	Monoclinic	$\text{mMnO}\cdot\text{MnO}_2\cdot\text{nH}_2\text{O}$	35~60	Granular	4.4~4.7	Common	Sedimentation
Newkirkite	Monoclinic	$\text{Mn}_2\text{O}_3\cdot\text{H}_2\text{O}$	62.4	Column	4.2~4.3	Rare	Sedimentation
Hausmannite	Tetragonal	Mn_3O_4	72	Granular	4.84	Common	Denaturation
Braunite	Tetragonal	Mn_2O_3	69.6	Granular	4.7~5.0	Common	Denaturation
Rhodochrosite	Trigonal	MnCO_3	47.8	Granular	3.6~3.7	Common	Sedimentation
Alabandite	Equiaxial	MnS	63.1	Block	3.9~4.1	Common	Sedimentation

90 As a vital strategic mineral resource, the manganese ore is widely used in steel, non-ferrous metallurgy,
 91 chemical, electronics, batteries, agriculture, medicine, and other fields (Figure 1). Based on the latest USGS
 92 2022 data (Figure 2a and Table 2), manganese ore reserves (by metal content) are mainly located in South
 93 Africa (about 640 million tons, 43%), Brazil (about 270 million tons, 18%), Australia (about 270 million tons,
 94 18%), Ukraine (about 140 million tons, 9%), Gabon (about 61 million tons, 4%), China (about 54 million tons,
 95 4%), and India (about 34 million tons, 4%) (USGS 2022). The global manganese ore resources are abundant,
 96 but the distribution of resources is uneven, and the ore grade varies significantly among these regions. The
 97 manganese-rich ore is concentrated in South Africa, Gabon, Brazil, India and Australia, whose grades are
 98 generally 35 to 50% (USGS 2022). However, Ukraine, China and Ghana are dominated by low-grade
 99 manganese ores, whose grades are mostly below 30%. Regarding manganese ore production (Table 2 and
 100 Figure 2b), the global manganese ore production in 2020 was about 18.9 million tons, with South Africa
 101 producing 6.5 million tons, accounting for nearly 30% of the total global manganese ore production. The global
 102 manganese ore consumption in 2021 once exceeded 20 million tons, of which South Africa produced 7.4
 103 million tons, accounting for 37% of the global production. Gabon and Australia produced 3.6 million tons and
 104 3.3 million tons, respectively, at 18% and 16%. In 2021, China became the fourth largest producer of
 105 manganese ore in the world, producing 1.3 million tons and having a 7.5% market share (USGS 2022).



106
 107 Figure 1. Simplified structure of the manganese industry chain. According to the grade of manganese ore, the formation
 108 process of manganese-based products can be recognized clearly. According to the difference in manganese content,
 109 different varieties of manganese ore can be divided into poor and rich ore. The differentiated manganese ore is prepared
 110 by the thermal and wet methods to achieve high-efficiency utilization of manganese ore. The figure of > 97% indicates
 111 that manganese used in iron and steel industry and battery industry accounts for more than 97% of industrial utilization
 112 of manganese ore.



113
 114 Figure 2. Latest global manganese ore distribution characteristics (a) Reserves distribution in 2022 (b) Production
 115 distribution in 2020 (USGS 2022).

Table 2. Mine production and reserves in the world (data from USGS 2022)

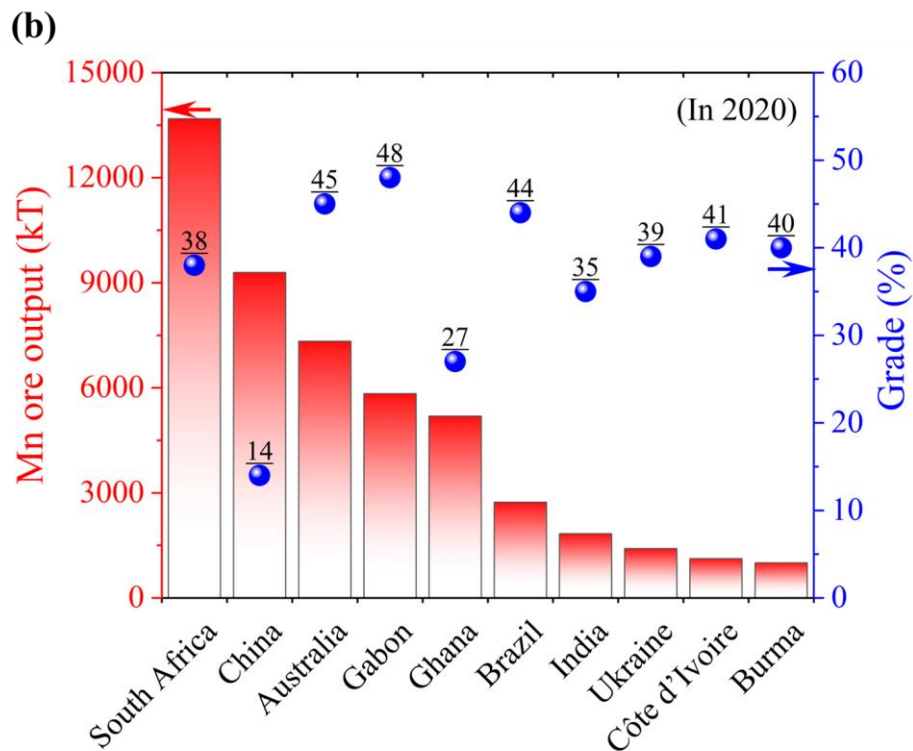
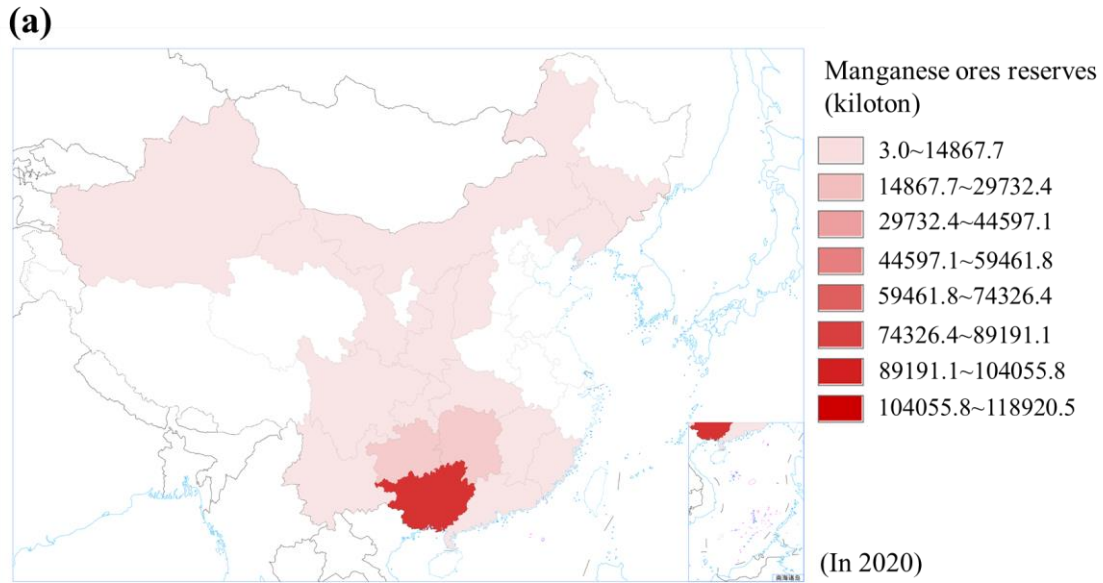
Countries	Mine production (kton)								Statistics of reserves (kton)							
	1995	2005	2015	2016	2017	2018	2019	2020	1997	2007	2017	2018	2019	2020	2021	2022
United states	-	-	-	-	-	-	-	-	-	-	-	-	-	-	-	-
Australia	1070	1450	2450	2240	2820	3480	3180	3330	30000	73000	91000	94000	99000	100000	230000	270000
Brazil	905	1590	1090	1080	1160	1310	1740	494	21000	25000	116000	120000	110000	140000	270000	270000
Burma	-	-	-	-	-	207	430	254	NA	NA	NA	NA	NA	NA	NA	NA
China	1000	1100	3000	2330	1700	1200	1330	1340	40000	40000	43000	48000	54000	54000	54000	54000
Côte d'Ivoire	-	-	-	-	-	395	482	525	NA	NA	NA	NA	NA	NA	NA	NA
Gabon	895	1290	2020	1620	2190	2330	2510	3310	45000	20000	22000	20000	65000	61000	61000	61000
Georgia	150	-	-	-	-	200	116	186	7000	NA	NA	NA	NA	NA	NA	NA
Ghana	-	-	416	553	810	1360	1550	637	NA	NA	12000	13000	13000	13000	13000	13000
India	627	640	900	745	734	961	801	632	24000	93000	52000	34000	33000	34000	34000	34000
Kazakhstan	-	-	222	212	168	140	140	158	NA	NA	5000	5000	5000	5000	5000	5000
Malaysia	-	-	201	266	478	390	390	347		NA	NA	NA	NA	NA	NA	NA
Mexico	174	180	220	206	212	210	202	198	4000	4000	5000	5000	5000	5000	5000	5000
South Africa	1350	2100	5900	5300	5400	5800	5800	6500	370000	32000	200000	200000	230000	260000	520000	640000
Ukraine	1100	770	410	425	735	517	500	578	135000	140000	140000	140000	140000	140000	140000	140000
Vietnam	-	-	-	-	-	-	158	121	NA	NA	NA	NA	NA	NA	NA	NA
Others	309	1390	678	681	898	397	270	260	Small	Small	Small	Small	Small	Small	Small	Small
Total	7580	10500	17500	15700	17300	18900	19600	18900	680000	440000	690000	680000	760000	810000	1300000	1500000

117 Note: NA stands for not available.

118 1.2 Distribution of manganese ore reserves and production in China

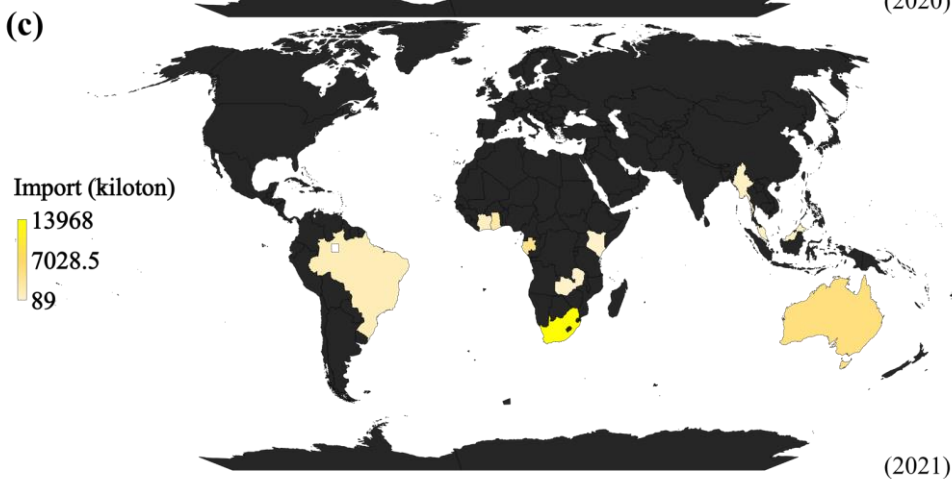
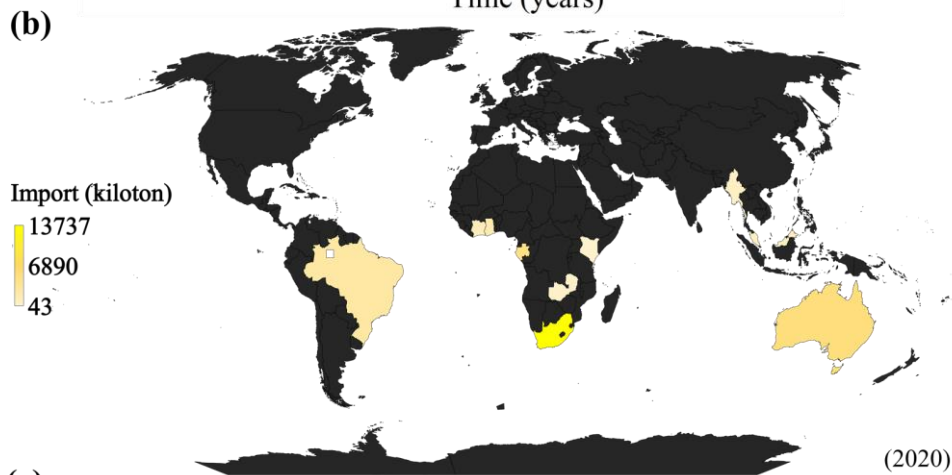
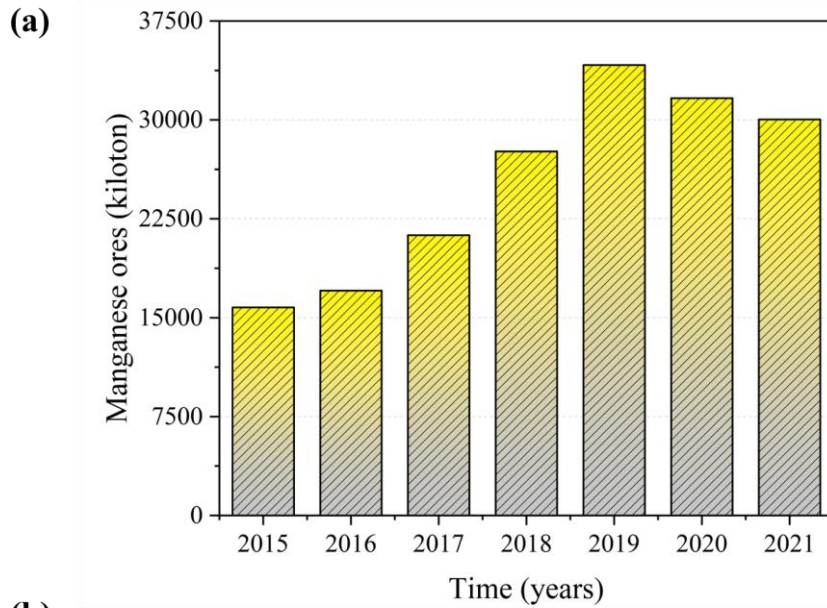
119 China has included manganese in the national strategic reserve during the 11th Five-Year Plan (Duan et
120 al. 2010). In China, manganese ore deposits are primarily concentrated in Guizhou, Guangxi, and Hunan
121 provinces. According to the "China Mineral Resources Report (2021)" released by the Ministry of Natural
122 Resources, China has identified 213 million tons of manganese ore reserves by the end of 2020 (China Mineral
123 Resources, 2021). There are 31.72 million tons more than in 2019, making it the second most valuable metal
124 mineral reserve after bauxite (Figure 3a). The industrialization of manganese-based cathode materials is
125 speeding up due to the rapid advancement of modification technology, which means that the high demand for
126 manganese in the steel industry and the high growth of manganese batteries will cause the dichotomous pattern
127 of the manganese industry. The manganese ore reserves in China are only one-fifth of those in South Africa,
128 which is ranked first in terms of manganese content until 2021, and the average manganese ore grade is only
129 21.4%, while that of the world's major manganese resource countries is approximately 40% (Figure 3b).

130 In contrast, the grade of manganese ore in China is much lower than in other major manganese ore
131 resource countries. In the metallurgical industry, manganese ore can be divided into rich and poor according
132 to the high or low manganese content, and the finished ore with manganese content above 30% is called rich
133 manganese ore in China. Low-grade manganese ore resources cannot meet the development demand, and
134 China is highly dependent on manganese ore imports. According to statistics in 2021, the import quantity of
135 manganese ore and its concentrate in China reached 30.03 million tons (Figure 4), with the discovery of four
136 world-class mega manganese deposits and one mega manganese rich deposit in Guizhou in 2021, recording
137 about 60% of all manganese ore resources in China. In addition to promoting Guizhou to become the largest
138 manganese ore deposit in China, this discovery could also alter the pattern of manganese ore deposits in China
139 and worldwide. Although the discovered manganese ore resources are still of low grade, their large reserves
140 make China the country with the largest manganese ore reserves in the world. Therefore, the manganese ore
141 resources in China are characterized by polarization between the rich and the poor regarding mineral grade
142 and rich in quantity (China Mineral Resources, 2021).



143

144 Figure 3. Distribution of manganese ore reserves in 2020 (a) Specific distribution of manganese ore reserves in China.
 145 Guangxi, Hunan and Guizhou are the three provinces with the richest distribution of manganese ore. (b) Global output
 146 and corresponding grade of manganese ore resources. The manganese ore grade is 14% in China, which is much lower
 147 than in other countries with an average grade of about 40% (Data from China Mineral Resources, 2021). The symbol unit
 148 of kT stands for kiloton.



149

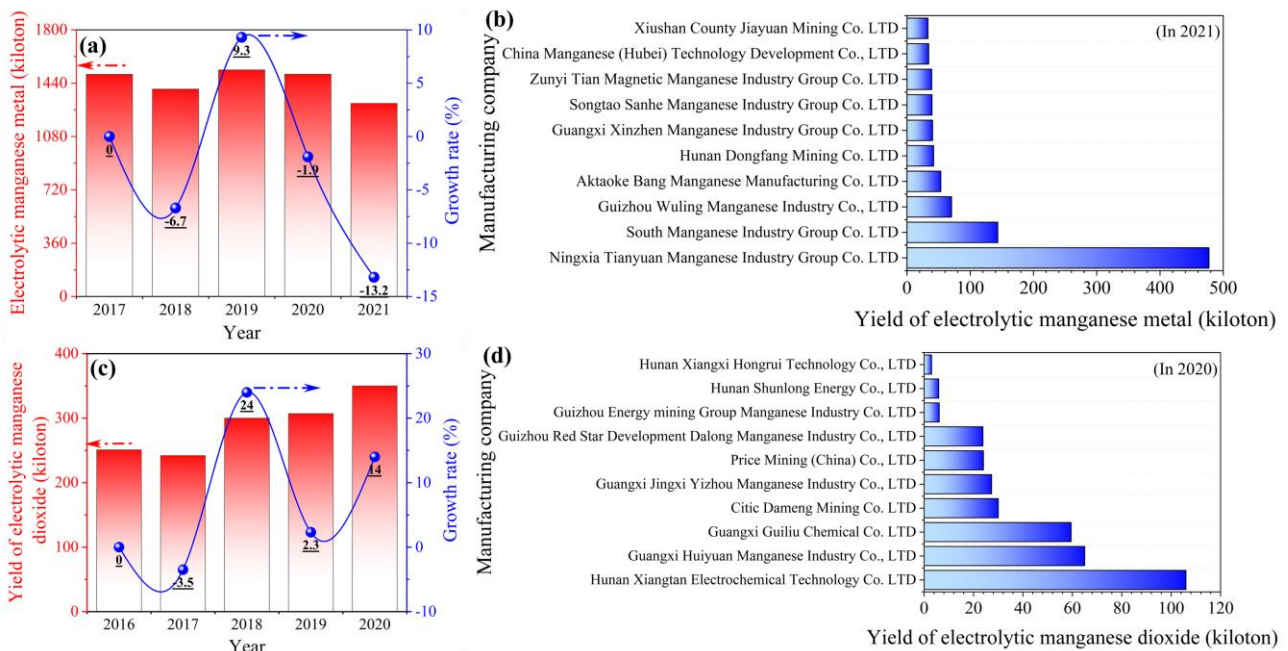
150 Figure 4. Global import distribution of manganese ore and its concentrates in China. (a) The import quantity of manganese
 151 ore resources from 2015 to 2021. The import quantity of manganese ores increased first and then decreased, and the
 152 maximum import quantity was the largest in 2019. (b) Global distribution of China's imported manganese ore in 2020 (c)
 153 Global distribution of China's imported manganese ore in 2021 (China Mineral Resources, 2021). The manganese ore
 154 imports from China are mainly concentrated to East Africa, Australia, Brazil and other countries.

155 1.3 Production and resource distribution of electrolytic manganese

156 Over 90% of manganese ores are processed to prepare manganese alloy products, mainly including
 157 ferromanganese alloy, silicomanganese alloy and manganese metal. In particular, ferromanganese alloy and
 158 silicomanganese alloy are mainly processed by high-grade manganese oxide ore. In 2020, China produced
 159 11.77 million tons of silicomanganese alloy, 1.89 million tons of ferromanganese, and 1.5 million tons of
 160 electrolytic manganese (China Mineral Resources, 2021) (Figure 5). Therefore, China is the country with the
 161 highest levels of both production and consumption of manganese alloy.

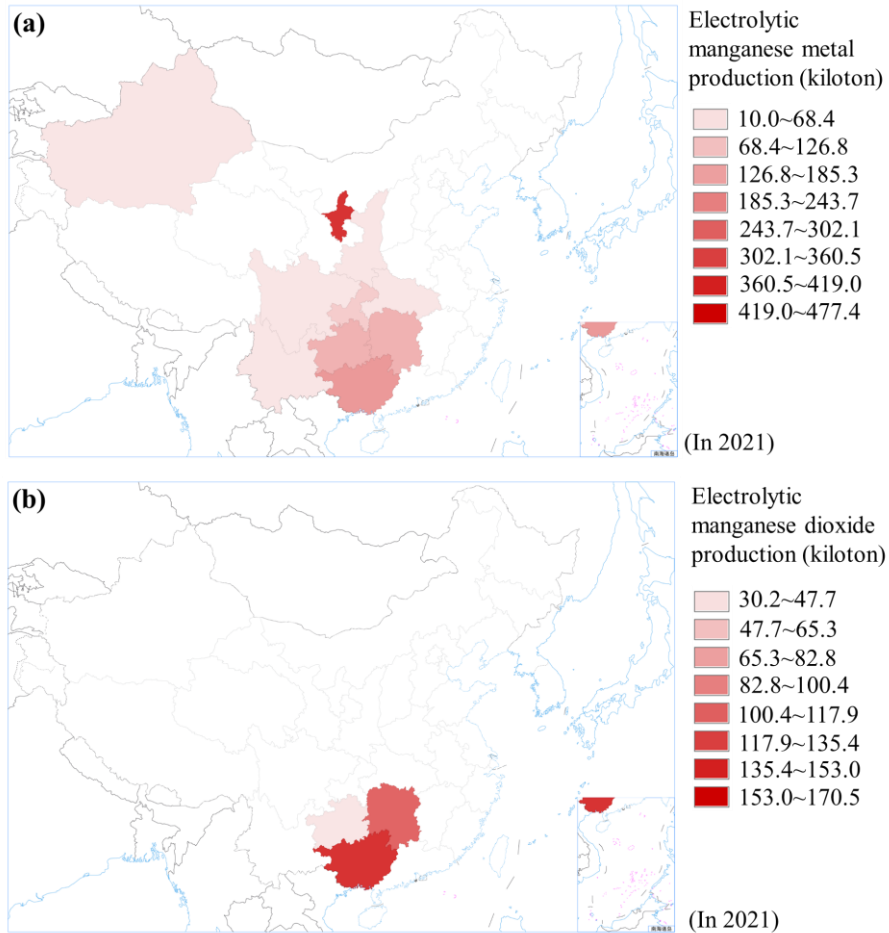
162 Electrolytic manganese is extracted from manganese ore by acid leaching and is subsequently
 163 electrolyzed and precipitated in an electrolytic cell. More precise data show that the output of manganese ore
 164 in China was 1.3 million tons in 2021, while the output of electrolytic manganese reached 1.304 million tons
 165 in 2021 (Figure 5). As a result, the production of various downstream manganese products depends upon
 166 imported high-grade manganese ore owing to the low grade of the manganese ore produced locally. The import
 167 dependence of manganese ore in China is consistently above 90%, and the import volume of manganese ore
 168 reached 29.968 million tons in 2021, with the external dependence as high as 95.7%. Due to the increase of
 169 "double control of energy consumption", the price range of electrolytic manganese and electrolytic manganese
 170 dioxide in China was 220% and 90%, respectively, in 2021 (Figure 6).

171 An essential component of electrolytic manganese is electrolytic manganese dioxide, the production of
 172 which has grown significantly since 2020. In 2020, the production of electrolytic manganese dioxide reached
 173 351,000 tons, an increase of 14.3% over the previous year. Driven by the demand of downstream primary
 174 battery enterprises, the output of the electrolytic manganese dioxide market increased significantly in 2020
 175 (Figure 5). In addition, the market demand for electrolytic manganese dioxide has grown significantly due to
 176 the sustained increase in the shipment of lithium manganate materials. In this regard, Xiangtan Electrochemical
 177 Group, the largest producer of electrolytic manganese dioxide, produced 106,000 tons in 2020, accounting for
 178 over 30% of the total domestic output with a significant scale advantage (China Mineral Resources, 2021).



179 Figure 5. Annual production and main production units of electrolytic manganese in China. (a) Production and growth
 180 rate of electrolytic manganese metal from 2017 to 2021. The maximum output of electrolytic manganese metal occurred
 181

182 in 2019. (b) Top ten electrolytic manganese metal production units in China in 2021. At present, the largest production
 183 site of electrolytic manganese metal is Ningxia Tianyuan Manganese Industry Group Co. Ltd. (c) Yield and growth rate
 184 of electrolytic manganese dioxide from 2016 to 2020. The maximum output of electrolytic manganese metal occurred in
 185 2020. (d) Top ten electrolytic manganese dioxide production units in China in 2020. Currently, the largest production site
 186 of electrolytic manganese dioxide is Hunan Xiangtan Electrochemical Technology Group Co. Ltd.



187
 188 Figure 6. Spatial distribution characteristics of electrolytic manganese in China. (a) Yield spatial distribution of
 189 electrolytic manganese metal in 2021. Ningxia, Guangxi and Hunan province have become the main electrolytic
 190 manganese metal production. (b) Yield spatial distribution of electrolytic manganese dioxide in 2021. Guangxi, Hunan
 191 and Guizhou provinces are the main production areas of electrolytic manganese dioxide.

192 1.4 Formation and stockpiling of Mn-rich residue

193 The process from manganese ore to the final manganese product is closely related to the target demand
 194 and the grade (manganese content) of the original ore. Most of the rich manganese ores containing at least 30%
 195 manganese are smelted by a pyrometallurgical process to be used in the metallurgical industry. The mining of
 196 poor manganese ores is often closely linked to the wet smelting process. Among the manganese electrolytic
 197 products, electrolytic manganese metal and electrolytic manganese dioxide belong to the manganese chemical
 198 processing products. With 93.6% of the manganese ore resources in China classified as poor, electrolytic
 199 manganese is the most significant manganese-based target product.

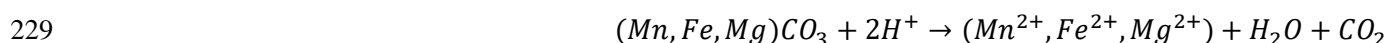
200 At present, there are two kinds of manganese metal production in the world consisting of wet metallurgy,
 201 such as the electrolytic method and pyro smelting, including electric silicon thermal and aluminium thermal

202 methods (Liu et al. 2019). The aluminium-thermal method consumes more aluminium, has a high cost, and
203 needs to use rich manganese ore as raw material. Meanwhile, the electro-silicon thermal method requires a
204 high grade of manganese ore and obtains manganese metal with low purity and a complicated process. The
205 electrolytic method of manganese sulfate solution is highly manipulable and not limited by low-grade
206 manganese ore resources. However, the electrolytic process known as leaching-separation-electrodeposition
207 can obtain electrolytic manganese ore with purity $\geq 99.8\%$ using low-grade (8–15%) manganese ore. Thus, it
208 is widely used in the electrolytic manganese ore industry. Therefore, wet metallurgy production has become
209 the primary way of manganese metal production. Almost all electrolytic manganese metal is manufactured in
210 South Africa and China, of which China accounts for more than 97% of the total electrolytic manganese metal.

211 Electrolytic manganese, including electrolytic manganese metal and electrolytic manganese dioxide,
212 uses raw manganese ore via acid leaching to form manganese-contained salt and then electrolytic precipitation
213 (He et al. 2021b). The production process of electrolytic manganese is shown in Figure 7, with further
214 elaboration as follows:

215 1) Taking manganese carbonate ore as an example, the block manganese ore is crushed and ball-milled into
216 manganese powder with a particle size of about 100 mesh. About 9 tons of manganese ore with 14% purity are
217 consumed to produce one ton of electrolytic manganese. However, manganese dioxide ores and reducing
218 substances are mixed in closed heating to reduce the tetravalent manganese to bivalent manganese to prepare
219 electrolytic manganese. The divalent manganese obtained from the reduction is crushed and prepared into the
220 above manganese powder for subsequent disposal.

221 2) Preparation of manganese sulfate solution. The electrolytic anode solution (H_2SO_4 , $40\text{ g}\cdot\text{L}^{-1}$) from the reflux
222 plant is introduced into the leaching tank. Then, a certain amount of sulfuric acid solution is added and mixed
223 with the prepared manganese ore powder. The manganese ore powder in the mixture reacts with sulfuric acid
224 to produce a manganese sulfate solution (Equation 1). Different from the process of preparing manganese
225 sulfate from manganese carbonate ore, manganese dioxide ore can prepare manganese sulfate solution by
226 reacting the prepared manganese dioxide powder with sulfuric acid. The other method for preparing sulfate
227 solution is through the redox reaction between manganese dioxide ore powder and sulfuric iron ore under the
228 action of sulfuric acid, which is usually defined as one-step mining of two ores.

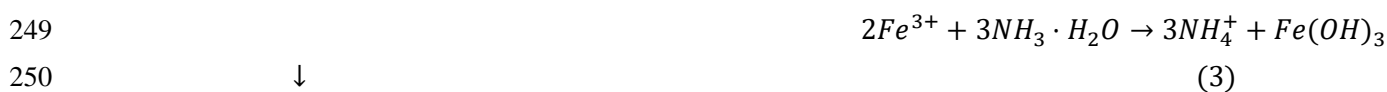


230
$$\uparrow \qquad \qquad \qquad (1)$$

231 3) The next step for electrolyte regulation. Due to the low potential of manganese, the electrolyte must maintain
232 a higher ammonium sulfate content to improve its hydrolysis pH and current efficiency. Specifically, the
233 mineral-to-acid ratio (mass ratio) for manganese carbonate ore powder leaching is 1: (0.55 ~ 0.6). The potential
234 effect is generating manganese ammonia ligand ions, which raises the hydrolysis pH of manganese ions and
235 improves the difficulty of hydrolysis. On the other hand, the added ammonium sulfate increases the solution
236 electrical conductivity and plays an excellent buffering role. Adding ammonium sulfate has a non-negligible
237 role in maintaining normal electrolysis operations. It is important to note that the amount of ammonium sulfate
238 added is related to the type of antioxidant used in electrolysis. In the case of selenium dioxide, the content of

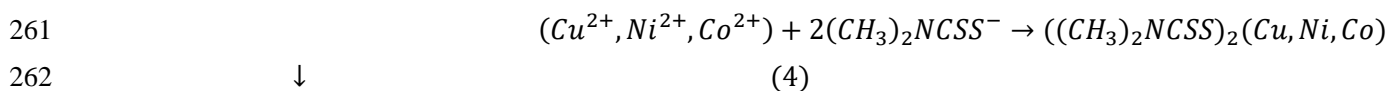
239 ammonium sulfate is usually 100-120 g·L⁻¹. As the selenium dioxide is replaced by sulfur dioxide, the content
240 of ammonium sulfate reaches 130-140 g·L⁻¹.

241 4) The part of electrolyte purification. A certain amount of soft manganese ore powder is added to the leaching
242 tank to oxidize the divalent iron in the manganese sulfate solution into trivalent iron (Equation 2). Then
243 ammonia is added to adjust the pH to 6.5–7.0. Therefore, the trivalent iron hydrolyzes to iron hydroxide
244 precipitates are removed (Equation 3). Most silica impurities also enter the leaching residues with the iron
245 hydroxide precipitation. A small amount of divalent manganese ions is also hydrolyzed and precipitated.



250 ↓
251 5) Solid-liquid separation of Mn-contained electrolyte. The solution delivered from the leaching tank is divided
252 into filtrates and residues after multiple pressure filtrations. The filtrates, also known as manganese sulfate
253 solution, are transferred to the sulfurization tank for deep impurity removal treatment. The residues as the
254 manganese sulfate acid leaching residues that is mostly disposed of by direct storage.

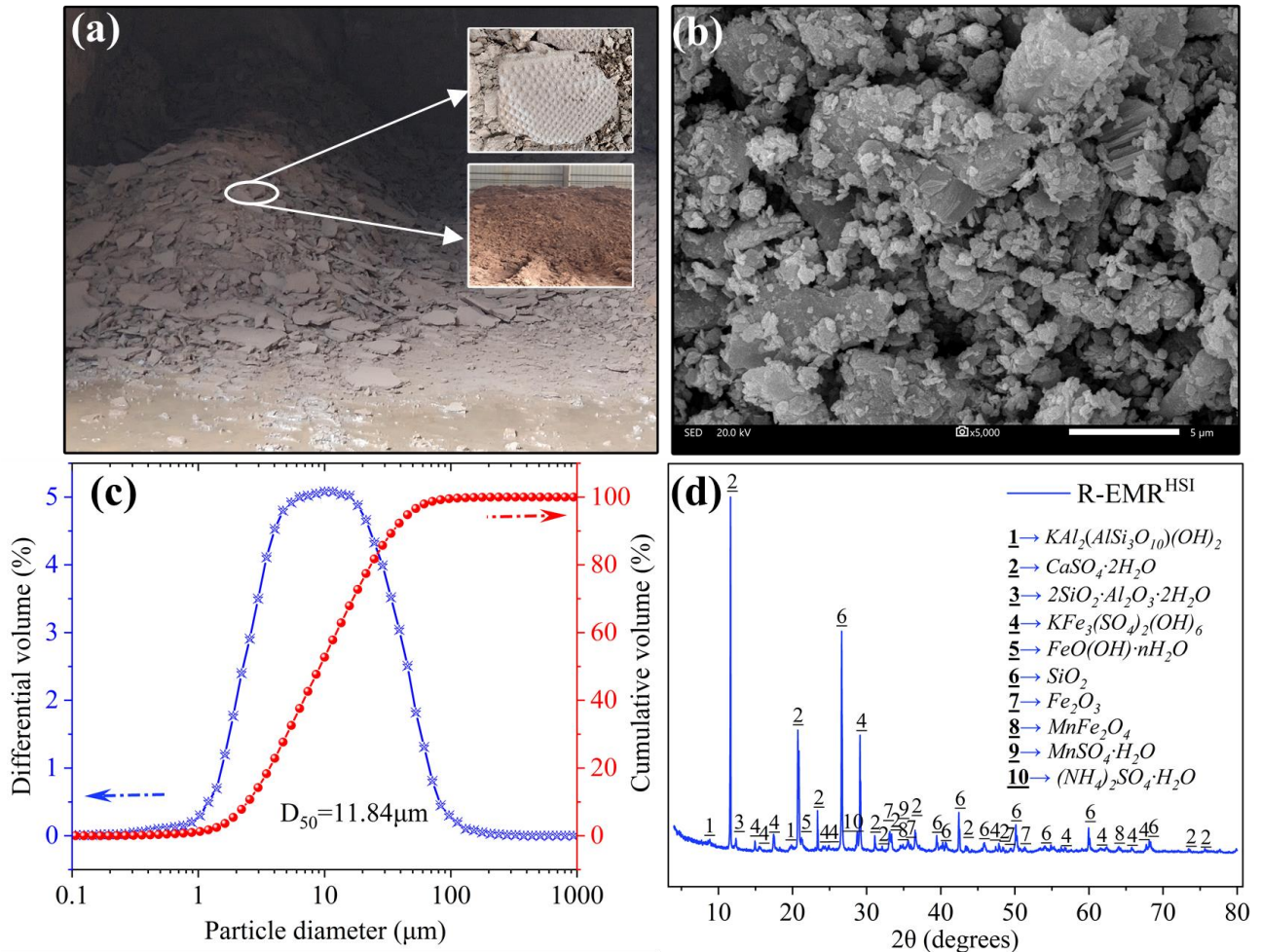
255 6) The treated step for heavy metals sulfurization and solid-liquid separation. The process is mainly completed
256 in the sulfurization tank. By adding sodium fumarate in the sulfurization tank, it generates sulfide precipitation
257 with copper, nickel, and other heavy metal ions in the manganese sulfate solution (Equation 4). Subsequently,
258 the sulfide precipitate generated in the sulfidation stage is passed by the filter press to complete solid-liquid
259 separation. The separated filtrate enters the settling tank, and the separated solid residues are sent to the residue
260 storage.



262 ↓
263 7) Static and fine filtration of the separated filtrate. The filtrate is finely filtered again by filtering equipment,
264 and then the selenium dioxide is added to the filtrate to prepare a qualified electrolyte. As described above, the
265 separated filtrate enters the electrolyzed tank and the separated solid filtrate is sent to the residue storage.

266 8) Electrolysis and post-treatment. In the electrolyzed tank, the electrolytic manganese metal and electrolytic
267 manganese dioxide will be deposited and precipitated from the cathode rod of the electrolyzed tank. Besides
268 precipitating oxygen on the anode, a certain amount of anode sludge will be generated. The residual manganese
269 ions and sulfuric acid in the anode solution are returned to the leaching tank for reuse. The manufactured Mn-
270 rich residue must undergo various processes once electrolysis is completed, including passivating, washing,
271 drying, and stripping. Specifically, 3% potassium dichromate is used for passivation to prevent the electrolytic
272 manganese from being oxidized in the air. The post-treatment process generates a certain amount of wastewater
273 containing manganese and chromium, which needs to be further treated.

300 rich residue can generally reach 43–73% (Table 3), and these ingredients are the main chemical components
 301 of building materials. Therefore, Mn-rich residue is a potential raw resource for construction materials.
 302 However, due to the employed hydrometallurgical process, Mn-rich residue contains many soluble harmful
 303 ions in addition to Mn^{2+} and NH_4^+-N .



304
 305 Figure 8. Characteristics of Mn-rich residue. (a) A large amount of Mn-rich residue tailing is deposited in tailings ponds,
 306 (b) the image of Mn-rich residue morphology obtained by 5000 times microscopic test. (c) particle size distribution curve
 307 of Mn-rich residue obtained by particle size analysis. The particle size D_{50} of Mn-rich residue after drying and sifting is
 308 11.84 μm. (d) mineral composition of Mn-rich residue obtained by diffraction technique. The label of R-EMR^{HSI} stands
 309 for the raw Mn-rich residue with high ferrum and silicon. The X-Ray Diffraction test result indicates that the main mineral
 310 phases of Mn-rich residue are gypsum, jarosite, and kaolin. Reprinted with permission of Elsevier from Wang et al.
 311 (2022a).

312 Meanwhile, the treatment method of Mn-rich residue is still mainly simple and crude, usually using a
 313 mulch landfill and building a reservoir or dam for disposal of stockpiling (He et al. 2021b). Despite establishing
 314 dumps or dams, Mn-rich residue poses significant environmental risks to the surrounding soil and water
 315 resources due to imperfect impermeability measures. Specifically, 1) On the open Mn-rich residue stockpiling,
 316 many abandoned Mn-rich residues occupy valuable land resources. The Mn-rich residue-based dumps are
 317 primarily adjacent to residential areas, encroaching on land for farming, forestry, industrial and mining
 318 purposes. Stockpiling of Mn-rich residues for a prolonged period may pose several hazards, including

319 environmental pollution, dam breakage, restrictions on regular production and the long-term development of
320 industries. 2) The harmful Mn-rich residue pollutes the atmosphere and the surrounding water-soil
321 environment as the treatment of Mn-rich residue relies on open stockpiling. Sunlight and wind will make Mn-
322 rich residue with fine particles enter the atmosphere, seriously impacting the surrounding ecological
323 environment. 3) The vast scale Mn-rich residue dissolved by rainwater leaching to produce the leachate
324 pollutants, including sulfate, ammonia nitrogen, manganese, arsenic, mercury and selenium. The formed
325 pollutants cause severe environmental risks, leading to gas, water, and soil hazards. In addition, organic matter
326 is scarce in Mn-rich residue, mainly composed of minerals like calcium and magnesium. There is a negative
327 impact on the significant biodiversity of the area as a result of this. It is challenging for the injured ecosystem
328 to recover when biodiversity is lost. 4) Many abandoned Mn-rich residues are not further integrated and utilized,
329 which causes a waste of resources. The above results show again that a large amount of stockpiled Mn-rich
330 residue causes a huge environmental burden. Therefore, targeting the harmless treatment and resources high
331 value-added utilization of Mn-rich residue is urgent. Notably, reducing the total amount of Mn-rich residue by
332 improving the production efficiency of Mn-rich residue is the primary front-end treatment for Mn-rich residue
333 disposal. Harmless pretreatment of Mn-rich residue is a vital prerequisite for its resource-based reuse.
334 Therefore, the reduction, pretreatment and high-value-added utilization of Mn-rich residue can solve the
335 current issue of manganese resource shortage and bring great environmental and economic benefits to society.
336 China's government has forced all electrolytic manganese companies to deal with Mn-rich residue. There has
337 been some effort to address this issue since the late 1990s, but there has not yet been a mature and reliable
338 industrial application (Duan et al. 2010). Mn-rich residue has thus grown to be a critical challenge in China
339 since it prevents the electrolytic manganese industry from developing sustainably.

340 Table 3. Major chemical compositions of Mn-rich residue from different Mn-rich residue stockpiling sites

No.	Country	Sites	Major composition (wt%)						Reference
			SiO ₂	SO ₃	CaO	Fe ₂ O ₃	Al ₂ O ₃	MnO	
1	China	Guizhou	26.22	36.63	18.97	7.79	3.00	5.21	Tian et al. 2019
2	China	Guizhou	33.75	20.61	14.03	5.07	8.99	3.94	Tang et al. 2019
3	China	Guizhou	31.38	18.58	9.45	7.35	10.71	4.82	Zhang et al. 2019
4	China	Guizhou	29.74	29.59	14.71	5.85	6.86	6.47	Chang et al. 2020
5	China	Guizhou	31.49	25.6	12.85	4.09	7.07	3.51	Huang and Zhang, 2022
6	China	Guizhou	27.60	33.97	18.90	3.58	8.21	2.34	He et al. 2022a
7	China	Guizhou	20.27	26.64	11.48	2.50	6.38	1.92	He et al. 2022b
8	China	Guizhou	29.63	29.54	14.82	5.41	8.32	2.02	Wang et al. 2022a
9	China	Guizhou	25.17	35.87	16.99	3.81	7.30	3.32	Duan et al. 2021
10	China	Guizhou	23.14	33.06	21.54	5.25	6.88	5.90	Shu et al. 2021
11	China	Guizhou	39.97	23.39	10.43	5.30	12.32	3.05	Shu et al. 2020a
12	China	Guizhou	37.56	22.95	16.93	4.78	12.14	3.12	Shu et al. 2020b
13	China	Guizhou	32.15	31.78	12.56	5.36	7.68	N.D	Chen et al. 2020a
14	China	Guizhou	32.32	30.77	14.27	6.32	7.63	3.00	Shu et al. 2018a
15	China	Guizhou	35.52	19.84	10.09	8.04	11.43	5.15	Xu et al. 2019
16	China	Guangxi	38.75	10.80	1.30	14.94	8.12	6.40	Li et al. 2018

17	China	Guangxi	30.79	18.24	7.68	3.13	9.18	N.D	Hou et al. 2019
18	China	Guangxi	27.62	28.07	16.52	10.97	2.89	10.41	Zhou et al. 2021
19	China	Guangxi	23.40	24.70	13.20	9.10	3.10	4.20	Lan et al. 2021a
20	China	Guangxi	35.20	9.38	1.19	15.17	7.85	6.14	Li et al. 2021
21	China	Guangxi	23.99	25.92	10.53	7.24	2.56	4.67	Lan et al. 2021b
22	China	Guangxi	22.30	36.88	13.22	9.40	3.20	4.65	Li et al. 2020a
23	China	Guangxi	23.41	34.22	15.45	10.79	2.60	9.60	Xue et al. 2020
24	China	Guangxi	23.99	n.d.	10.53	7.24	2.56	4.67	Lv et al. 201
25	China	Guangxi	24.80	25.70	16.20	13.10	5.10	4.75	Lan et al. 2019a
26	China	Guangxi	23.40	27.60	15.00	8.60	6.50	4.80	Li et al. 2019a)
27	China	Guangxi	23.41	27.58	14.96	8.57	2.46	4.80	Li et al. 2019b
28	China	Guangxi	38.75	10.80	1.32	14.94	8.12	6.40	Li et al. 2018
29	China	Hunan	34.67	20.53	5.58	21.21	9.01	3.94	Wang et al. 2022
30	China	Hunan	35.04	21.37	8.67	20.54	5.97	N.D	Li et al. 2016
31	China	Hunan	31.80	32.20	12.60	5.80	7.60	2.30	Liu et al. 2013
32	China	Hunan	24.60	37.80	8.60	7.90	12.20	4.60	Li and Zhang, 2020
33	China	Hunan	44.10	5.54	6.05	2.81	23.74	12.00	Yu et al. 2019
35	China	Hunan	24.60	N.D	8.60	7.90	12.20	4.60	Li et al. 2015a
36	China	Hunan	24.60	22.00	8.59	7.87	12.15	10.90	Wu et al. 2015
37	China	Chongqing	32.32	32.77	15.10	5.62	7.01	2.42	Shu et al. 2019a
38	China	Chongqing	40.08	22.72	7.34	5.58	13.78	2.99	Wang et al. 2020
39	China	Chongqing	34.65	26.40	14.78	7.01	8.21	3.02	Shu et al. 2016
40	China	Chongqing	27.93	37.31	15.39	5.29	5.78	5.05	Du et al. 2015
41	China	Chongqing	61.24	3.86	11.57	3.97	11.36	0.82	Chen et al. 2021
42	China	Chongqing	36.40	19.60	13.10	5.83	9.37	N.D	Zhan et al. 2020
43	China	Chongqing	34.40	26.80	13.00	6.12	7.85	N.D	Zhan et al. 2018
44	China	Chongqing	32.32	30.77	14.27	6.32	7.63	3.00	Shu et al. 2017
45	China	Chongqing	17.17	19.89	8.85	3.89	5.03	3.05	Wang et al. 2016
46	China	Chongqing	22.03	31.37	19.16	8.83	3.09	8.54	Du et al. 2014a

341 Note: N.D stands for not detected.

342 1.6 Potential of resource utilization of Mn-rich residue as building materials

343 The entire society has progressively agreed that environmental conservation is necessary to ensure
344 human living standards and advance the resource - efficient development of the national economy and society
345 (Rodrigues et al. 2022; He et al. 2022b; Wang et al. 2022a). As the main environmental protection content, the
346 tri-wastes treatment and comprehensive utilization is a vital pivot to purify the living environment and protect
347 the ecological balance. Given the huge amount of Mn-rich residue, a high efficiency and low environmental
348 impact approach for utilizing and disposing of Mn-rich residue is urgently needed. However, the over-
349 quantification of harmful substances and low reactivity of Mn-rich residue have caused adverse effects, which
350 hinder the development of the resource utilization of building materials. The existing results indicate that the
351 cycle usage amount of Mn-rich residue is small and the properties of cement cementitious materials made by
352 Mn-rich residue are dissatisfactory. The requirements of the current rapid industrialization cannot be fulfilled

353 in the existing context. Therefore, the cyclic utilization of Mn-rich residue is the top priority in its treatment
354 procedure.

355 Due to the electrolysis, purification and deposition process, Mn-rich residue contains many
356 aluminosilicate, hematite, quartz, gypsum, jarosite and kaolin for potential development into a construction
357 material (Duan et al. 2011; He et al. 2021a). Therefore, how to turn Mn-rich residue into treasure and realize
358 the high value-added resource utilization of Mn-rich residue-based building materials is worth further
359 investigation. As far as we know, most of the current reviews and studies focus on the direct or indirect resource
360 utilization of Mn-rich residue, which promotes the treatment of Mn-rich residue to a certain extent. The Mn-
361 rich residue is rich in silicon, aluminium, iron, calcium, sulfur, and other chemicals, which means that Mn-rich
362 residue, as a misplaced resource, is also a promising artificial mineral material. Meanwhile, the building
363 materials industry is experiencing a mineral resource shortage, causing it to struggle to find suitable and
364 alternative mineral resources. The current treatment of Mn-rich residue still presents some concerns, including
365 high costs, low efficiency, limited resource utilization, and disposal method. The benefits of the substantial
366 amounts of aluminosilicate, quartz, hematite, gypsum, and other components in Mn-rich residue are not fully
367 exploited by the existing resource exploitation. The misplaced resources will likely be wasted again if the value
368 of waste to wealth is low. Therefore, Mn-rich residue still has substantial utilization potential and disposal
369 value in China. It is urgent for Mn-rich residue to be utilized in a harmless and high-value-added manner. As
370 of yet, there has not been a systematic review of Mn-rich residues that are utilized in high-value-added
371 applications. This paper comprehensively compares and analyses the most advanced technologies of Mn-rich
372 residue in fountainhead reduction, pretreatment and high value-added utilization. In conjunction with current
373 Mn-rich residue production and treatment technology, the industrial application reveals the barriers to
374 recycling and reusing Mn-rich residue. The benefits and drawbacks of the existing Mn-rich residue processing
375 and disposal technologies are discussed, along with practical solutions for achieving high value-added resource
376 utilization of Mn-rich residue. This work supports realizing the sustainable development and environmental
377 protection strategy of Mn-rich residue.

378 **2. Mn-rich residue reduction and safe storage technology**

379 This section primarily focuses on the fountainhead reduction of Mn-rich residue, which is the first
380 premise of its effective long-term management. Mn-rich residue fountainhead reduction mainly refers to
381 reducing the initial production of Mn-rich residue as much as possible, thereby reducing its impact on the
382 ecosystem at the source. Specifically, the reduction of Mn-rich residue is mainly reflected in optimising the
383 hydrometallurgical process and purifying the original manganese ore.

384 **2.1 Improvement of manganese ore grade**

385 The impurities such as phosphate, silica-aluminium phase and iron and associated metals such as nickel,
386 zinc, and copper, which are difficult to separate, cause the significant difference between the reserves of
387 manganese ore and the amount of manganese resources. Therefore, reducing the impurity of manganese ore
388 and realizing the enrichment of manganese resources can effectively decrease the yield of Mn-rich residue.
389 The main challenge is to improve the manganese richness of manganese ore and reduce the impurities in
390 manganese ore. Meanwhile, the methods to improve manganese ore grade mainly focus on physical enrichment,
391 such as water washing, gravity separation, magnetic separation, flotation, and microwave heating (Xie et al.

2021a). The coupled methods also can be formed to improve its enrichment efficiency. Table 5 lists the fountainhead reduction results of Mn-rich residue using the physical method to improve manganese ore grade. As the initial procedure, the water washing removes clay minerals from manganese ore, which provides a prerequisite for the subsequent operations. Gravity separation screens manganese minerals based on mineral density difference and the reported maximum enrichment rate of MnO reached 91.1% (Muriana, 2015). However, due to the negligible density difference between the Fe-Mn minerals (Table 4), the gravity separation for iron and manganese minerals is insignificant. Therefore, high-intensity magnetic separation has become a wall-breaking technology for sorting Fe-Mn minerals.

After high-intensity magnetic separation, manganese can be concentrated to more than 45% and Mn sorting index is close to 90% (Tripathy et al. 2015). However, the single magnetic separation for manganese and iron is still not ideal. Therefore, the flotation method consisting of some chemical substances is provided to achieve the manganese from Fe-Mn ores separation to some extent. The manganese grade can be raised from 10.7 to 18.3% and the sorting index can reach 97% using linoleic acid (Zhou et al. 2015). However, the slurry formed by flotation is overly complex with the dissolution of Mn^{2+} , Mn^{3+} , Fe^{2+} and Fe^{3+} ions. The oxidation-reduction and hydration of dissolved ions on the mineral surface deteriorate the flotation. In addition, the microwave heating method increased the manganese grade from 30 to 40% (Chen et al. 2017).

In conclusion, a single-treated method cannot deal with more and more complex manganese ore resources. In other words, this means that the multi-coupling method has great potential. When the combined treatment of high-gradient magnetic separation and wet-beneficiation, the manganese recovery efficiency can reach 64% and a purity of 97.9% $MnCO_3$ can be obtained (Zhang et al. 2017a).

Table 4. The density of various manganese-bearing minerals

Manganese-bearing minerals	Density (g cm ⁻³)	Manganese-bearing minerals	Density (g cm ⁻³)
Pyrolusite	4.7–4.8	Hematite	4.9–5.3
Psilomelane	4.4–4.7	Magnetite	4.9–5.2
Rhodochrosite	3.6–4.7	Siderite	3.7–4.0
Braunite	4.7–5.0	Limonite	4.0–4.3

Table 5. Summary of results of direct physical methods to improve the grade of manganese ore

Mn ores	Separation methods	Feed (wt.%)	Concentrates (wt.%)	Recovery (wt.%)	Reference
Nigeria	Gravity	25.36	56.13	95.18	Oyelola 2020
Nigeria	Wet gravity	NA	NA	91.11	Muriana 2015
Hunan, China	High-intensity magnetic	10.39	22.75	89.88	Wu et al. 2015
India	Two-stage magnetic	22.40	42.10	44.70	Tripathy et al. 2015
India	Single dry magnetic	27.33	35.52	44.00	Bhoja et al. 2021
Canada	Direct dry magnetic	26.00	49.00	69.00	Elliott 2020
India	Direct wet magnetic	32.42	42.00	47.00–49.00	Singh 2011
South Africa	High-intensity magnetic	29.80	29.72	59.90	Mpho et al. 2013

Note: NA stands for information not available. Mn recovery (wt.%) = Product weight (wt.%) × Product Mn grade (wt.%) / Feed Mn grade (wt.%)

2.2 Leachate enhancement by Mn^{2+}

417 After enhancing the manganese ore grade to reduce the final Mn-rich residue yield, the further operation
418 to achieve Mn-rich residue reduction is to improve the Mn^{2+} leaching efficiency in the leachate. The
419 improvement of leaching efficiency is closely related to the type of manganese ore. Manganese carbonate ore,
420 such as rhodochrosite, can be obtained directly by H_2SO_4 with a leaching efficiency of over 96% for Mn^{2+}
421 during the hydrometallurgical process (Liu et al. 2014). With the gradual depletion of manganese carbonate
422 ores with high grades, the recovery of manganese oxide ores, such as soft manganese ore, has become a matter
423 of concern. Therefore, mining low-grade soft manganese ore and low-grade manganese carbonate ore can
424 boost the amount of raw materials for electrolytic manganese metal production, and much attention has been
425 conducted to this territory. As stated above, soft manganese ores need to be converted from tetravalent to
426 divalent form before leaching by the introduced reducing substances to enhance the formation efficiency of
427 manganese sulfate solution.

428 The critical point for improving Mn^{2+} leachate is the selection of reducing and leaching agents. All
429 reducing agents in acidic environments effectively reduce tetravalent Mn to a divalent state, achieving the Mn
430 leaching value of over 90%. The addition of calcium sulfide can reach 95% Mn leaching efficiency by
431 converting MnO_2 to Mn_3O_4 (Li et al. 2015a). The sulfur dioxide translates Mn^{4+} into Mn^{2+} to realize the Mn
432 leaching rate of 95% (Sun et al. 2013). The Mn^{2+} leaching rate reached 96.6% as the SeO_2 was the reducing
433 agent (Ding et al. 2016). When using H_2O_2 as a reducing agent to improve the reducibility of acid-leaching
434 environment, the leaching rate of Mn^{2+} from low-grade manganese ores reaches 97%. The leaching rate of
435 divalent Mn from manganese ores can reach 95.6% using H_2SO_4 as leachate (Zhang et al. 2013). Introducing
436 lignin can realize the Mn leaching rate of 91% by reducing Mn^{4+} to Mn^{2+} via H_2SO_4 (Xiong et al. 2018). It is
437 noted that reducing agents, such as pyrite, must be utilized carefully with iron-bearing Mn ores because they
438 might introduce a lot of Fe ions into the leachate and dramatically raise the post-treatment cost. The electric
439 field has an excellent leaching efficiency but is seldom employed in production due to the problematic leaching
440 conditions, limited application, and expensive costs (Zhang et al. 2017b). In addition, the bioleaching method
441 is another good option for Mn^{2+} leaching because of its simple operation and low cost. The 99% Mn^{2+} leaching
442 rate can be obtained using microorganisms (Xin et al. 2015). Electrolytic manganese is not widely used in
443 bioleaching because it is time-consuming and more complex than other processes.

444 2.3 Improvement of the mineral separation degree and water content regulation

445 The following enhancement measure is to remove other impurities, such as iron from the manganese
446 sulfate solution, which is the main impurity in manganese ore. Since iron has similar chemical properties to
447 manganese, the iron phase needs to be eliminated before electrolysis to improve the purity of the manganese
448 sulfate solution (Liu et al. 2019). Iron ions are removed by adjusting the pH and forming $Fe(OH)_3$ to separate
449 them from the leach solution. Most impurity silica also precipitates with $Fe(OH)_3$ to constitute the leaching
450 residue during the iron deposition and separation. Some manganese ions are also partially precipitated into the
451 leaching residue. Therefore, stepwise graded filtration can remove heavy metals from Mn-rich residue by
452 leaching the residue. It is debatable that the huge added disposal costs directly limit the broad application of
453 this disposal process. However, this issue can be solved more effectively by directly separating the mineral
454 phase using chemical products or supplementary building materials as target products.

455 Based on the hydrometallurgy process of electrolytic manganese, finer manganese powder is used to

456 improve the leaching efficiency. It means that the particle size of the leaching residue is around 10–50 μm
457 (Wang et al. 2022a). The clay mineral contained in fine power has a multitude of interlayer waters. Meanwhile,
458 H_2SO_4 interacts with calcareous minerals to create extremely hydrophilic gypsum during leaching. The
459 $\text{Fe}(\text{OH})_3$ colloid deposited and separated during the leaching process also contains a lot of water. Therefore,
460 the above substances cause Mn-rich residue to have an extremely high moisture content of 20 to 35%. A large
461 amount of soluble manganese ions (2.0–5.0%), $(\text{NH}_4)_2\text{SO}_4$ (2.5–5.0%) and heavy metals such as Ni^{2+} , Co^{2+} ,
462 Cr^{6+}) are also stored in the water solution. The leading cause that makes Mn-rich residue capable of causing
463 significant contamination with these dangerous compounds. A point of concern is that nearly 10% of the
464 manganese is lost in the contamination process by soluble substances. Hence, the water content of Mn-rich
465 residue is relatively high in the case of direct disposal due to the storage of rainwater. Although the air-dried
466 Mn-rich residue is lumpy, it still contains a significant amount of chemically bound water. Since Mn-rich
467 residue contains a high amount of water, it is difficult to recover and recycle, while its high viscosity and
468 tendency to harden after evaporation prevents it from being readily mixed with other materials. In this manner,
469 controlling Mn-rich residue water content reduces the amount of Mn-rich residue and the potential ecological
470 risk as well as saving land resources. It has been reported that the use of surfactants such as dodecyl amine can
471 change the hydrophilicity of the Mn-rich residue particle surface and form a semi-micellar Mn-rich residue
472 surface, resulting in a significant reduction of water content. In addition, innovative filtration devices are
473 developed to facilitate the control of moisture content.

474 2.4 Limitations and future direction

475 There are several restrictions on the above-mentioned disposal methods, notwithstanding their ability to
476 decrease the volume of the Mn-rich residue stockpile. 1) First, due to the gradually increased complexity of
477 associated minerals in manganese ores, reducing the Mn-rich residue stockpile volume is challenging using
478 simple methods. There are relatively few works to develop coupled-composite beneficiation processes for this
479 issue. 2) In addition, due to the high-water content of Mn-rich residue and the residual of soluble materials, it
480 is necessary to innovate new preparation processes to reduce the stockpile volume of Mn-rich residue. As a
481 result, the cost of production is inevitably increased, which is unfavourable for business. In addition, the use
482 of foreign high-grade manganese ore also provides a potential option for Mn-rich residue fountainhead
483 reduction. However, the fountainhead reduction treatment of Mn-rich residue will become more prominent
484 with the increasing emphasis on the natural environment and the shortage of manganese ore resources with
485 high-grade. Mn-rich residue fountainhead reduction should be characterized as a complicated task, requiring
486 reduction of the water content in the Mn-rich residue, improvement of the manganese leachate purity, and
487 constant process control of the electrolytic manganese production. In addition, it is critical to ensure the Mn-
488 rich residue fountainhead reduction is conducted without contributing to secondary environmental damage.

489 The existing high-temperature reduction-smelting separation process is the most promising
490 pyrometallurgical process for separating ferromanganese from ores (He et al. 2021a; Wang et al. 2022a). The
491 difference in fusibility between silicate and ferrofluid or iron carbide is the key to manganese and iron
492 separation. In decades of successful manufacturing operations, the method has proven suitable for fully
493 utilizing ferromanganese ores. In addition, the separation process of carbon thermal reduction roasting is better
494 for the separation of manganese and iron in ferromanganese-based minerals. Alkaline additions can accelerate

495 the development of metallic iron during direct reduction thermal treatment and disassemble the structure of
496 irreducible silicates, which further enhances the reduction of ferromanganese oxides. Since the combined
497 reaction of manganese dioxide and sulfur is thermodynamically feasible, sulfate roasting or sulfur leaching is
498 a promising method for selective extraction from ferromanganese ores. Overall, it is recommended to use a
499 combination of various physicochemical approaches and thermal treatment processes to achieve a high-quality
500 realization of the fountainhead reduction of Mn-rich residue.

501 **3. Harmless pretreatments of Mn-rich residue**

502 The optimization of the metallurgical process and purification of the acid leachate can initially realize
503 Mn-rich residue fountainhead reduction. In practice, it is not feasible to interrupt the production of Mn-rich
504 residue by the filter-pressing operation, which entails that the subsequent disposal of the Mn-rich residue
505 stockpiled will require a new technology for disposal. As mentioned earlier, stockpile based Mn-rich residue
506 depletes land resources and causes environmental damage. The harmfulness of Mn-rich residue is attributed to
507 the heavy metal ions and ammonia nitrogen contained in the high-water content with high migration rates.
508 Therefore, in-situ Mn-rich residue pretreatment or synergistic control of the harmless and resource utilization
509 is required regardless of resource utilization or disposal in stockpiles.

510 The pretreated Mn-rich residue has the potential to construct building and industrial materials rather
511 than being a dangerous industrial solid waste material that endangers environmental safety. As such, the
512 harmless pretreatment of Mn-rich residue is an essential prerequisite to ensuring the efficient use of resources
513 which is often closely related to its utilization. Mn-rich residue treatment techniques can be classified into dry,
514 thermal, and wet disposal technologies according to their physicochemical characteristics.

515 **3.1 Direct dry disposal technology of Mn-rich residue**

516 The direct dry disposal technology of Mn-rich residue benefits from the introduction of additional
517 chemicals. The addition of chemical substances to the Mn-rich residue can achieve the immobilization of
518 harmful substances, but also improve its own chemical composition, and thus improve the reactivity. As part
519 of the stabilization-solidification process, soluble hazardous substances are transformed into insoluble and
520 chemically stable hazardous substances to reduce migration and diffusion (Kim and Lee, 2017; Salami et al.
521 2022). This method has the potential for the environmentally friendly disposal of solid waste in landfills,
522 providing a focused guide for direct dry disposal of Mn-rich residue. The stockpiled Mn-rich residue is mixed
523 with cementitious materials or selected chemical reagents to stimulate reactivity while providing long-term
524 safety and optimizing resource utilization. In addition, the effective stabilization of soluble heavy metal ions
525 in Mn-rich residue also somewhat reduces environmental pollution.

526 Currently, quicklime, magnesium oxide, silicate, phosphate, and cement are used as common curing
527 agents (Qiao et al. 2010; Silva et al. 2011; Cho et al. 2014; Zhang et al. 2018; Ouhadi et al. 2021; Hossain et
528 al. 2022). The main results are summarized as follows: 1) The alkaline environment provided by alkaline curing
529 agents such as quick lime and magnesium oxide allows the rapid removal of $\text{NH}_4^+\text{-N}$, while the soluble Mn is
530 cured to MnOOH and Mn(OH)_2 (Chen et al. 2019). 2) Intensive stabilisation of Mn^{2+} and removal of $\text{NH}_4^+\text{-N}$
531 from Mn-rich residue can be achieved using strong alkaline solutions such as sodium hydroxide. However, the
532 expensive treatment costs limit the widespread use of this technology. 3) Introducing low-grade chemical
533 reagents provides a more economical solution to the above limitation. Shu et al. (2020b) prepared a phosphate-

534 based binder to stabilize Mn^{2+} and NH_4^+-N in Mn-rich residue using a low-cost, low-grade MgO and calcium
535 super-phosphate. The leachate of phosphorite by-product as an inexpensive phosphate source was employed
536 to achieve high-quality stabilization of NH_4^+-N and Mn^{2+} in collaboration with MgO or CaO (Chen et al.
537 2020a). Although the economics and stabilization efficiencies were improved, the long-term service stability
538 of the formed condensation products and the optimal design of the disposal process continue to impede the
539 long-term development of this technology. In this regard, a stepwise stabilization and solidification strategy
540 was adapted for the high-quality disposal of Mn^{2+} and NH_4^+-N in Mn-rich residue (Shu et al. 2019b). Despite
541 the excellent removal efficiency of Mn^{2+} and NH_4^+-N , the long-life durability of the final products was not
542 effectively expressed. 4) The CaO-based solidification products were prevented from ageing owing to the
543 application of $CaCO_3$ and Na_3PO_4 . Additionally, carbon dioxide and alkaline additives were used to achieve
544 manganese carbonation fixation while reducing carbon emissions in the form of carbon capture (Chen et al.
545 2016; Baena-Moreno et al. 2022; Ho et al. 2022). The added CaO solidified the soluble manganese in Mn-rich
546 residue to $MnCO_3$, and the addition of $MgCl_2 \cdot 6H_2O$ and $Na_3PO_4 \cdot 12H_2O$ solidified NH_4^+-N in Mn-rich residue
547 to $MgNH_4PO_4 \cdot 6H_2O$.

548 In summary, the main principle of typical chemical reagent disposal for Mn-rich residue is to use the
549 selected alkaline oxides to regulate the pH value during the solidifying process and transforms soluble
550 manganese into insoluble manganese-based hydroxide and high-valent manganese oxide. The remaining
551 soluble manganese was solidified using different phosphorus-containing compounds, and magnesium ions in
552 Mn-rich residue hardened the NH_4^+-N into an insoluble phosphate. The adequate solidification of soluble Mn^{2+}
553 and NH_4^+-N can be achieved by modulating the molar ratios of compounds such as CaO, MgO, and P, as well
554 as the dissolution degree, thus providing a significant contribution to the improvement of the site safety index
555 of Mn-rich residue.

556 In addition, cement as a hydraulic cementitious material forms a dense microstructure by cement
557 hydration reaction, while the constructed microstructure enables high-quality curing of solid waste (Wang et
558 al. 2022b). The C-S-H gel phase generated during the cement hydration can adsorb and encapsulate Mn^{2+} . In
559 addition, $Ca(OH)_2$ formed from cement hydration reacts with Mn^{2+} to form $Mn(OH)_2$ precipitate. Since the
560 ammonium salts can be translated to dissociated ammonia in alkaline cement-based pastes or mortars, the
561 hydration heat release can accelerate the change of the dissociated ammonia to gaseous ammonia, which is
562 eventually released in the form of ammonia gas (Zhan et al. 2022). When the cement mass fraction was 25–
563 45%, the leaching concentration of manganese was still within the safe range under acidic conditions at a pH
564 of 2, even if the cement curing body was damaged during employing (Wang et al. 2022a). Li et al. (2016)
565 found that the soluble Mn content was reduced to 0.515 mg L^{-1} , attributed to the prepared cementitious material
566 with encapsulation properties by mixing cement with Mn-rich residue. Cement, synergistic quicklime and
567 waste fly ash were used to solidify Mn-rich residue, and the final toxic leachate Mn^{2+} concentration was only
568 0.022 mg L^{-1} (Zhan et al. 2018). In addition, red mud, calcium carbide slag, and furnace slag were also used
569 as coagulants to solidify soluble Mn in Mn-rich residue with a 99% solidification rate (Zhang et al. 2020),
570 resulting the solidified Mn including MnO_2 , Mn_2SiO_4 and $Ca_4Mn_4Si_8O_{24}$. In addition, He et al. (2022b)
571 successfully stabilized Mn-rich residue using alkaline burning material, a by-product of the cement industry.
572 The high-activity substances form C-S-H gel and ettringite with good ionic substitution and encapsulation on

573 heavy metal ions.

574 In short, the co-curing of cement and other chemicals can further improve the curing effect of Mn^{2+} and
575 NH_4^+-N in Mn-rich residue. Unfortunately, the high disposal costs and strength losses present a significant
576 obstacle to the development and application of co-curing technology. Although industrial byproduct substitutes
577 have reduced the cost of Mn-rich residue processing, the additional ions carried by the byproducts increase the
578 complexity of the curing system. In response to the decline in the grade of Mn ore resources, the components
579 of Mn-rich residue become increasingly complex. The complex environment in which Mn-rich residue
580 products are cured severely challenges their long-term durability. As the chemicals introduced into the Mn-
581 rich residue curing body become more complex, the stability of the product is also being challenged.
582 Consequently, the more complex phase composition creates an ever-present environmental risk for the curing
583 environment. While this was taking place, the project focused primarily on the safe and stable development of
584 the Mn-rich residue stockpile site and did not fully consider the potential application of Mn-rich residue due
585 to a lack of consideration for the use of resources.

586 3.2 Wet disposal technology of Mn-rich residue

587 The wet disposal technology does not conflict with the extraction of iron and manganese elements in
588 Mn-rich residue fountainhead reduction but is a win-win strategy that complements each other. The main
589 difference between Mn-rich residue fountainhead reduction and the wet disposal process for Mn-rich residue
590 harmless disposal lies in the disposal goal. The former is to minimize the final Mn-rich residue yield, while
591 the latter mainly serves for safe stockpile disposal and resource utilization. With the decline in mineral storage
592 and grades, re-leaching recovery and electroremediation technology have emerged as a new hotspot for Mn-
593 rich residue development to reach sustainable development and reduce tailings waste (He et al. 2021c). Re-
594 leaching recovery disposal is mainly focused on water leaching, acid leaching, alkaline leaching and
595 bioleaching. The content of Mn^{2+} and NH_4^+-N decreases with increasing stockpile time, which indicates that
596 these soluble compounds are leached out by dissolving with rainwater flushing (Velusamy et al. 2021).

597 The water leaching technology is mainly used to recover Mn^{2+} ions and NH_4^+-N through water or
598 enhanced water washing (Huang et al. 2022). It has been shown that 1) Water leaching can recover soluble
599 manganese from Mn-rich residue. The kinetic leaching process is controlled by the diffusion of Mn ions in
600 Mn-rich residue with crystalline phases such as SiO_2 and $CaSO_4 \cdot nH_2O$ ($n=0.5$ and 2). The temperature and
601 liquid-solid ratio boost can enhance extractive efficiency (Zheng et al. 2020). 2) The primary water leaching
602 efficiency is only near 80%, and multiple water leaching can increase the leaching efficiency again to more
603 than 90%. The total recovery of soluble ions increases significantly with an increasing number of washes
604 (Wang et al. 2018). 3) The traditional mixed water washing method was changed to mixed water with filter
605 cake and the manganese recovery reached 95.82% after six times water-washing. 4) Enhanced water leaching
606 can significantly improve leaching efficiency. A combination of calcination and multiple water washing was
607 used by He et al. (2020) to achieve high-efficiency disposal of Mn^{2+} ions and NH_4^+-N , resulting in an Mn^{2+}
608 concentration of 0.005 mg L^{-1} .

609 In contrast to water leaching, acid leaching is also an environmentally safe common wet disposal
610 technology (Chen et al. 2022). In particular, acid leaching involves the application of sulfuric acid,
611 hydrochloric acid, nitric acid, and some organic acids to destroy the mineral structure of an ore material under

612 specific conditions. By converting the target matter into acid-soluble ions, this method enables the efficient
613 extraction of valuable elements from the ore. The results of existing Mn-rich residue acid leaching shown that
614 1) a single acid leaching can achieve efficient leaching and recovery of Mn. About 20 wt% H₂SO₄ was used at
615 90 °C for 3 h to leach manganese with a leaching efficiency of 96% (Peng et al. 2013). This indicates that acid
616 leaching helps to enhance the recovery of Mn²⁺ and NH₄⁺-N. 2) Enhanced acid leaching technique can further
617 improve the leaching efficiency of Mn-rich residue. The 1.67 M H₂SO₄ solution at 85 °C in conjunction with
618 0.2 M H₂C₂O₄ was performed to finish the leach and the leaching efficiency of Mn under this effect achieved
619 99.9%. However, Mn-rich residue could not be recovered in large quantities using the water and acid leaching
620 techniques due to the low solubility of silica and silicate in acidic environments.

621 Alkaline leaching can be used to recover silica resources for secondary use. The alkaline leaching studies
622 show that 1) silicon resources can be leached from Mn-rich residue using a common sodium hydroxide solution
623 at 130 °C for 5 h, achieving a leaching efficiency of 82.04%. 2) The leaching behavior of silicon in Mn-rich
624 residue in an alkaline environment follows the contraction nucleation model controlled by interfacial chemical
625 reactions. It was determined that the problem could be addressed by leaching the washed Mn-rich residue with
626 40 wt% NaOH at 140 °C for 12 h and adding the synthesized polyamide to form mesoporous silica (Zhang et
627 al. 2017c).

628 Bioleaching has more potential for using industrial solid waste due to its mild reaction conditions,
629 feedstock adaptability and high target selectivity (Lv et al. 2021a). The bioleaching results show that: 1) The
630 suitable microorganisms can achieve high leaching efficiency while accomplishing the target elements. Sulfur-
631 oxygen and iron-oxygen microorganisms were used to leach Mn-rich residue. The combined leaching
632 efficiency of Mn attained 99.7% (Duan et al. 2011; Lan et al. 2021c). 2) Bioleaching technology has different
633 differentiation and decomposition abilities for minerals and can be recovered into regulated phases by acid-
634 base adjustment. 3) Bioleaching technology contributes well to enriching and extracting silicon resources
635 (Chen et al. 2021). The bacteria were isolated from Mn-rich residue and stored in residue yards, with molasses
636 being used as the carbon or nitrogen source for bacterial growth. The pH of the solution was adjusted to 8.5-
637 9.0, which resulted in complete bioleaching that can achieve leaching and recovery of S, Mn, Mg, Fe, and
638 NH₄⁺-N (Lan et al. 2019). However, the leaching technology is accompanied by the intervention of a large
639 amount of solution, which means there is a risk of secondary contamination of the leachate. The high disposal
640 cost and low disposal efficiency hinder the further advancement of leaching technology.

641 Electroremediation technology is widely used as a more desirable physical remediation method for
642 disposing of contaminated soils and industrial wastes. The target contaminants are transferred into unique
643 solutions by electro-migration and electro-osmosis to achieve contaminant remediation (Chen et al. 2020b). In
644 contrast to the extraction of valuable materials, this technology is primarily concerned with removing and
645 disposing of hazardous waste. Shu et al. (2019c) used deionized water and H₂SO₄ solution as the anode
646 electrolyte and cathode electrolyte and added sodium dodecylbenzene sulfonate and oxalic acid as electric field
647 enhancers in Mn-rich residue. The removal efficiency of Mn²⁺ and NH₄⁺-N reached 94.74% and 88.20%,
648 respectively. The electroremediation promoted the decomposition of complex salts such as (NH₄)₂(Mg, Mn,
649 Fe)(SO₄)₂·6H₂O. The Mn²⁺ ions moved from the cathode to the anode region, eventually forming Mn(OH)₂
650 and MnOOH, while NH₄⁺-N transported from the cathode to the anode region, respectively, where they

651 eventually solidified as $(\text{NH}_4)_2\text{SO}_4$ on the Mn-rich residue surface. As a result, the utilization of electric field
 652 disposal has significantly improved the distribution of ions on the surface of Mn-rich residue particles and
 653 promoted the dissolution of phases containing Mn^{2+} and $\text{NH}_4^+\text{-N}$ (Yang et al. 2021; Li et al. 2022a; Deng et al.
 654 2021). Shu et al. (2016a) employed a 9.2 wt% H_2SO_4 solution with $\text{FeSO}_4\cdot 7\text{H}_2\text{O}$ to leach the Mn-rich residue
 655 by an enhanced electric field, resulting in an Mn leaching rate of 96.2%. Other literature indicated that: 1) The
 656 Fe^{2+} added and improved electric field might boost Mn leaching efficiency by more than 50%. 2) Optimizing
 657 the electric field parameters, including increasing H_2SO_4 concentration, decreasing the reacted intensity,
 658 extending the reacted time, and synergistically adding a surfactant, may improve the final leaching rates of
 659 Mn^{2+} and $\text{NH}_4^+\text{-N}$. In addition, the multi-step collaboration wet disposal of Mn-rich residue can improve the
 660 leaching efficiency of detrimental substances. The physicochemical synergies promote the high-quality
 661 disposal of Mn-rich residue. However, the complexity of the process reduces the universality of disposal and
 662 increases the cost of disposal. The development of multifield coupling processing technology with high
 663 adaptability, low cost, and low power consumption requires further exploration and research.

664 3.3 Fire roasting disposal of Mn-rich residue

665 Fire roasting technology is one of the most metallurgically mature extraction techniques compared to
 666 other disposal methods that still need further development. It provides a high-temperature environment where
 667 other chemicals are mixed in a given atmosphere. The target minerals can be efficiently extracted by converting
 668 the difficult-to-separate raw materials into easily separable or soluble raw minerals. Table 6 shows the
 669 equations and required temperatures for the sulfate calcination and reduction roasting reactions in Mn-rich
 670 residue. It can be seen that calcination above 600 °C decomposes the sulfate into SO_2 and oxidizes Mn^{2+}
 671 Mn_3O_4 , Mn_2O_3 and MnO_2 .

672 The decomposition temperature of common sulfate in the Mn-rich residue can be reduced by adding an
 673 appropriate amount of reducing carbon powder. When high-temperature calcination or roasting is performed,
 674 the Mn-rich residue can be stimulated to improve the feasibility and availability of resource utilization.
 675 Currently, fire roasting technology has been widely used to treat sub-stable industrial solid waste. For Mn-rich
 676 residue, 90.75% of Mn elements can be recovered by a two-step roasting operation. Mn-rich residue also
 677 exhibits high pozzolanic activity after calcination due to the continuous generation of glassy materials. This
 678 offers infinite possibilities for utilizing Mn-rich residue as a high-valued resource (Wang et al. 2022a). Notably,
 679 the undue energy consumption and increased carbon emission caused by fire roasting technology significantly
 680 limit its popularization in the harmless stage of Mn-rich residue. Harmless disposal caused by fire roasting
 681 does not involve high value-added stimulation of resource utilization because it can realize both harmless and
 682 resource utilization. Compared with harmless treatment, fire roasting contributes more to effectively utilizing
 683 Mn-rich residue resources. The Mn-rich residue resource utilization part further elaborates the specific
 684 summary and analysis.

685 Table 6 The sulfate calcination and reduction roasting reactions in Mn-rich residue

Direct high-temperature calcination disposal process	
$2(\text{NH}_4)_2\text{SO}_4 = 4\text{NH}_3 (\text{g}) + 2\text{SO}_2 (\text{g}) + 2\text{H}_2\text{O} (\text{g}) + \text{O}_2 (\text{g})$	$T \geq 600 \text{ } ^\circ\text{C}$
$4\text{MnSO}_4 = 2\text{Mn}_2\text{O}_3 + 4\text{SO}_2 (\text{g}) + \text{O}_2 (\text{g})$	$T \geq 970 \text{ } ^\circ\text{C}$
$3\text{MnSO}_4 = \text{Mn}_3\text{O}_4 + 3\text{SO}_2 (\text{g}) + \text{O}_2 (\text{g})$	$T \geq 980 \text{ } ^\circ\text{C}$

$\text{MnSO}_4 = \text{MnO}_2 + \text{SO}_2 (\text{g})$	$T \geq 1120 \text{ }^\circ\text{C}$
$2\text{MgSO}_4 = 2\text{MgO} + 2\text{SO}_2 (\text{g}) + \text{O}_2 (\text{g})$	$T \geq 1040 \text{ }^\circ\text{C}$
$2\text{CaSO}_4 = 2\text{CaO} + 2\text{SO}_2 (\text{g}) + \text{O}_2 (\text{g})$	$T \geq 1670 \text{ }^\circ\text{C}$
The process of high temperature calcination of reductive substances	
$2(\text{NH}_4)_2\text{SO}_4 + \text{C} = 4\text{NH}_3 (\text{g}) + 2\text{SO}_2 (\text{g}) + 2\text{H}_2\text{O}(\text{g}) + \text{CO}_2 (\text{g})$	$T \geq 240 \text{ }^\circ\text{C}$
$4\text{MnSO}_4 + \text{C} = 2\text{Mn}_2\text{O}_3 + 4\text{SO}_2 (\text{g}) + \text{CO}_2 (\text{g})$	$T \geq 420 \text{ }^\circ\text{C}$
$3\text{MnSO}_4 + \text{C} = \text{Mn}_3\text{O}_4 + 3\text{SO}_2 (\text{g}) + \text{CO}_2 (\text{g})$	$T \geq 530 \text{ }^\circ\text{C}$
$2\text{MgSO}_4 + \text{C} = 2\text{MgO} + 2\text{SO}_2 (\text{g}) + \text{CO}_2 (\text{g})$	$T \geq 310 \text{ }^\circ\text{C}$
$2\text{CaSO}_4 + \text{C} = 2\text{CaO} + 2\text{SO}_2 (\text{g}) + \text{CO}_2 (\text{g})$	$T \geq 850 \text{ }^\circ\text{C}$

686 3.4 Constraints and future directions for the harmless disposal of Mn-rich residue

687 The harmless treatment of Mn-rich residue is a prerequisite for resource utilization that mainly involves
688 the extraction of valuable elements and the high-quality elimination of hazardous elements. Some studies have
689 proposed relatively suitable solutions for the environmentally friendly treatment of Mn-rich residue, but the
690 current disposal methods are still limited due to the increase of Mn-rich residue emissions caused by the
691 mineral complexity of Mn-rich residue and the reduction of manganese ore grade. The harmless treatment of
692 Mn-rich residue is closely related to its reduction and resource utilization. There is a limited way in which
693 direct dry disposal can fully utilize the value-added of Mn-rich residue since it is usually restricted to the
694 consumption of highly hazardous elements. This means that Mn-rich residue is often disposed of as worthless
695 waste. Mn-rich residue contains a large amount of calcium, aluminium, silicon, iron, sulfur and other elements
696 and their oxides and minerals based on the mineral composition. Therefore, in the hazardous-free disposal of
697 Mn-rich residue, harmful elements should be selectively absorbed and other harmless mineral elements should
698 be retained to contribute to the high-value resource utilization of Mn-rich residue.

699 The wet disposal technology can realize the high-efficiency extraction of valuable elements in Mn-rich
700 residue through the dissolution-leaching-filtration process. The use of high-efficiency extraction is closely
701 linked to the regulation of the leaching parameters, which in turn results in an excessive quantity of leaching
702 liquid and a significant risk of secondary contamination. In spite of the fact that electroremediation offers a
703 reasonable solution to these problems, its continued development is limited by the efficiency of this technology,
704 the secondary treatment of electrolytes, and the economic feasibility. The calcination technique can activate
705 Mn-rich residue while achieving harmless disposal, which implies that Mn-rich residue can be subjected to
706 resource utilization rather than inert waste. Despite this, the release of gas and the consumption of energy
707 during the calcination process inhibit the promotion of this technique. In order to resolve this issue, co-
708 calcination technology could be adopted in the development of Mn-rich residue calcination. Specifically, the
709 exhaust gas from calcined Mn-rich residue can be collected using a gas collection device and transformed into
710 chemicals or reducing gases for demand. Physicochemical excitation is applied before the Mn-rich residue is
711 calcined to maximize its activity. The utilization of Mn-rich residue will be maximized when it is processed
712 into high-active resource minerals such as fly ash and slag. Therefore, the development of an evaluation system
713 between Mn-rich residue activity and energy consumption, economic cost and disposal efficiency would
714 significantly impact the progression of environmentally sound disposal of Mn-rich residue.

715 4. Resource utilization of Mn-rich residue

716 The resource utilization of Mn-rich residue after harmless disposal is the key procedure to realize the
717 transformation of waste into treasure. The Chinese government supports using industrial waste residues in
718 manufacturing construction materials such as brick, cement clinker, concrete skeleton, and ceramsite as long
719 as they adhere to national regulations to promote the holistic reuse of waste resources (Figure 9). Mn-rich
720 residue has much potential for use in construction materials since its main phases, quartz, aluminium silicate,
721 iron phase, and gypsum, where all of these belong to the CaO-SiO₂-Al₂O₃-Fe₂O₃-CaSO₄ compositions (Wang
722 et al. 2023). This section mainly summarizes and critically analyzes the specific components of Mn-rich
723 residue resource utilization, which will help improve the efficiency of Mn-rich residue.

724 4.1 Building materials resource utilization of Mn-rich residue based on chemical component regulation

725 4.1.1 Aluminosilicate phase

726 Following the 11th Five-Year Plan national circular economy development goals in China, the "Notice
727 of the General Office of the State Council on further promoting wall material innovation and energy-saving
728 Buildings" was issued. The use of non-clay bricks based mainly on industrial solid waste has been considerably
729 encouraged. However, with economic development and living standard improvement, public awareness of
730 environmental protection has become increasingly widespread. In addition, clay brick has some
731 insurmountable defects such as high energy consumption, high pollution, and waste of cultivated land.
732 Therefore, using solid waste to prepare wall materials effectively realizes resource utilization, brings economic
733 benefits, and substantially reduces environmental pollution. The Mn-rich residue contains many silicon and
734 aluminium elements, promoting the stable development of its resource utilization. The resource utilization in
735 building materials of the aluminosilicate phase from Mn-rich residue mainly focuses on brick and roadbed
736 materials. Previous studies have shown that Mn-rich residue can be mixed with lime to achieve manganese
737 fixation and ammonia removal, and then the treated Mn-rich residue is combined with cementitious material
738 and sand aggregate to produce baking-free bricks under high-pressure steam (Zhou et al. 2014; Du et al. 2014a
739 and 2014b). All the indexes and toxic leaching test results meet the requirements when the Mn-rich residue
740 content is 30%, the cement content is 10.5%, the sand and stone aggregate content is 59.5%, the forming
741 pressure and vapor pressure are 25 MPa and 1.2 MPa, respectively. When the proportion of Mn-rich residue,
742 cement, aggregate and water is 25%, 20%, 30% and 25%, respectively, the compressive and flexural strength
743 properties of the non-burning brick are 16.40 MPa and 3.19 MPa, respectively. Li et al. (2020b) mixed calcium
744 hydroxide, heat-activated feldspar powder and Mn-rich residue to make a billet and treated it for 2 h under
745 forming pressure of 20 MPa and steam temperature of 160 °C. The maximum compressive strength of the
746 steam brick was 23.5 MPa. The above studies showed that SiO₂ in Mn-rich residue reacted with calcium
747 hydroxide to form hydrated calcium silicate under high-temperature steam conditions.

748 The Mn-rich residue, cement and slag were also mixed to form non-firing permeable bricks (Wang et al.
749 2019). After 28 days, the strength of 3.53 MPa and the permeability of $3.2 \times 10^{-2} \text{ cm s}^{-1}$ were higher than the
750 demand for standard. The inside hole morphology of the Mn-rich residue-based porous brick was examined
751 utilizing industrial computer tomography (Tang et al. 2019). The results showed that its optimum permeability
752 coefficient prepared with 6 MPa forming pressure was $3.3 \times 10^{-2} \text{ cm s}^{-1}$. Unlike non-burning bricks, the
753 calcinated Mn-rich residue has excellent pozzolanic activity and can be used as a brick-making base material.
754 As sintering temperatures increase, brick loss on ignition and shrinkage rates increase, but porosity and water

755 absorption decline while brick strength and density increase significantly. The compressive strength of sintered
756 bricks prepared by mixing Mn-rich residue with shale and fly ash can reach 22.64 MPa, and the manganese
757 concentration in leachate decreases from 451.08 to 0.68 mg L⁻¹ (Zhang et al. 2011). Roadbed material has
758 excellent raw material adaptability since it is used as an infrastructure material (Qiao et al. 2010). Zhang et al.
759 (2019) used Mn-rich residue, calcium carbide slag and red mud to prepare the subgrade materials with 7 days
760 of unconfined compressive strength up to 5–7 MPa. The concentration of NH₄⁺-N and Mn²⁺ in the leaching
761 solution collected from subgrade materials was lower than the threshold of groundwater quality standard. In
762 conclusion, the above studies were focused on the resource reuse of the Mn-rich residue aluminosilicate phase
763 in building materials. The use of aluminosilicate in Mn-rich residue as a wall and roadbed material expands
764 the scope of Mn-rich residue applications and improves its utilization efficiency.

765 4.1.2 Resource utilization of sulfate phase in Mn-rich residue

766 The Mn-rich residue is rich in sulfate, which is as high as 15~25% in the SO₃ state. When Mn-rich
767 residue is added to cement concrete as a mixture or admixture, its sulfate-rich properties cannot be fully
768 exploited. The pozzolanic activity of sulfate-activated fly ash is defined as a fly ash-lime-sulfate system.
769 Sulfate can change the arrangement structure of fly ash particles and activate the active SiO₂ and Al₂O₃ in fly
770 ash effectively (Nandhini et al. 2022; Priyadarshi et al. 2023). By increasing its solubility, the activity of
771 pozzolanic ash can be stimulated. The soluble sulfate in Mn-rich residue can better stimulate the pozzolanic
772 activity of fly ash and lime and can be used as the mixture or admixture by taking full advantage of its sulfate-
773 rich property. Calcium oxide was used to dissolve and dehydrate Mn-rich residue to prepare the fly ash
774 activator, which could stimulate the hydration activity of low-grade fly ash and produce the concrete composite
775 admixture. The adverse effects of manganese slag can be minimized by adding the appropriate amount of waste
776 stone powder.

777 In addition, Mn-rich residue can also be employed to enhance the pozzolanic properties of the calcined
778 slag. The roasting-activated Mn-rich residue, calcium hydroxide and cement clinker were mixed as an activator
779 to prepare slag-based cement (Wang et al. 2013). The carbide slag also can be employed to prepare cement
780 binding material by mixing it with Mn-rich residue and blast furnace slag (Xu et al. 2019). With the increased
781 calcium hydroxide dosing in the formed binding materials, the sulfate in Mn-rich residue contributes to the
782 depolymerization and hydration of blast slag. The pore refinement enhances the structural compactness of the
783 product and significantly reduces heavy metals in Mn-rich residue. In a crystalline structure of silico-oxygen
784 and alumina-oxygen bonds, a portion of silicon is substituted by heavy metal ions. The PI 32.5 cement
785 threshold was attained by the composite cementitious material created.

786 The strength of the composite made by Mn-rich residue is also better than that of PI 42.5 cement after
787 activating Mn-rich residue with an alkaline activator. The prepared sample remarkably cures Cd, Pb, Mn, Zn
788 and other heavy metals in Mn-rich residue. The Mn-rich residue was also utilized as a sulfate activator to
789 promote the pozzolanic properties of steel slag. When mixed Mn-rich residue with steel slag instead of 40%
790 cement, the strength of the formed cement samples was significantly higher than that of the non-Mn-rich
791 residue activated materials. Additionally, the cement based on Mn-rich residue can achieve the strength
792 requirements of PI 42.5 when the replacement content of cement is increased to 50% with 14% Mn-rich residue.
793 As a means to further reduce cement content, the ground Mn-rich residue, alkali metal hydroxides, and furnace

794 slag were mixed to produce composite binding materials (Wang et al. 2020). Cementing material prepared with
795 45% Mn-rich residue has a 28-day strength property of 30 MPa and an excellent Mn curing property.

796 In the process of cement production, gypsum can be employed to regulate the serviceability of products.
797 Due to the hydrometallurgy processing, the Mn-rich residue contains a certain amount of gypsum dihydrate
798 phase and shows a remarkable effect as retarding agent. For Mn-rich residue without calcination, it belongs to
799 inert silica-aluminium material with extremely rich sulfate content and inactive SiO₂ (about 20–40%). As a
800 result, the early mechanical properties of Mn-rich residue-doped cement are lower than those of natural
801 gypsum dihydrate cement produced by the abundant SO₃ and additional parts of inactive substances. Based on
802 the small differences in the late strength between Mn-rich residue-doped cement and natural gypsum dihydrate,
803 it is apparent that the overall effect of Mn-rich residue is similar to natural gypsum dihydrate as a cement
804 retarder. In addition, the sulfate in Mn-rich residue mainly exists in various forms, such as gypsum dihydrate,
805 ammonium sulfate, and manganese sulfate. Adding a certain amount of quick lime in Mn-rich residue is
806 conducive to converting other forms of sulfate into gypsum dihydrate to provide more favourable conditions
807 for its use as a cement retarder.

808 In conclusion, the resource utilization of sulfate in Mn-rich residue is due to the excitation effect of
809 sulfate. Therefore, adding activated Mn-rich residue as high-activity sulfate activators in cooperation with
810 other active materials can prepare low-carbon and high-powered supplementary cementitious materials. As a
811 result, the utilization efficiency of sulfate in Mn-rich residue is improved, and the amount of recycles disposed
812 of in Mn-rich residue is increased. As a result of reduced cement usage, carbon emissions from cement are
813 diminished.

814 4.1.3 Resource utilization on multiple-phase oxides in Mn-rich residue

815 Ceramics are more commonly used in construction than cement because of their superior mechanical
816 properties, outstanding acid and alkali resistance, and workability. Since Mn-rich residue contains the main
817 components for the preparation of ceramics (CaO, SiO₂, Al₂O₃, and Fe₂O₃), Na, K, Mg and other alkali metal
818 ions, it can be used as a flux during the production to reduce the sintering temperature of the prepared ceramics.
819 Qian et al. (2012) melted Mn-rich residue and ground it into less than 150 μm particle size powder with water
820 quenching and cooling to prepare matrix glass powder. The ceramics with excellent crystallization activation
821 energy were then obtained by mixing the matrix glass powder with a polyethylene glycol solution. Jiang et al.
822 (2020) successfully prepared Mn-rich residue-based glass ceramics with 1% porosity, 40% sintering shrinkage
823 and 425 MPa micro-hardness by high-temperature calcination. The prepared glass-ceramics have a good
824 immobilization effect on manganese ions in Mn-rich residue, and the toxic concentration of the leaching
825 solution is much less than the prescribed limits.

826 The combination of Mn-rich residue with carbonite, kaolin, and dolomite at 1100 °C and 3 MPa forming
827 pressure produced porous ceramics with a porosity of 69.7%, a strength of 6.97 MPa, and good pH tolerance
828 (Wu et al. 2016). As a result of using Mn-rich residue and talc as the primary processing materials and then
829 adding suitable bauxite and quartz, it is possible to prepare ceramics with a high bending strength of 105 MPa
830 when heated at 1100~1200 °C (Wu et al. 2013). Ceramic bricks with low water absorption, high volume density
831 and good performance were prepared by sintering Mn-rich residue and waste glass at 900 °C. The water
832 absorption rate and compressive strength of reclaimed ceramic wall brick prepared by Mn-rich residue and

833 waste ceramic grinding powder are 0.75% and 25.2 MPa (Wang et al. 2013). The mechanical properties of the
834 porous materials decrease with the increase in silicon carbide content. Zhan et al. (2021) produced lightweight
835 ceramide by sintering the mixture of Mn-rich residue, fly ash, and cleaned fly ash at 1160 °C, plus a holding
836 time of 12 min. The product possesses a good curing effect on heavy metal elements in raw materials (Zhan et
837 al. 2021).

838 Cement-based cementitious materials are the main infrastructure construction material, and their
839 preparation involves a certain amount of clay minerals and other ore resources. With the development of
840 urbanization, increasing infrastructure construction has put forward higher requirements for producing
841 necessary cement-based cementitious materials. However, large raw material ore consumption limits cement-
842 based cementitious material output development. The use of industrial waste residue to replace clay, sand and
843 ore in part or whole realizes the effective utilization of industrial waste residue as resources. Additionally, it
844 lessens the usage and waste of these resources as well as the harm caused by ore mining to the environment.
845 Mn-rich residue contains rich elements such as silicon, iron, aluminium, calcium and sulfur, which are
846 consistent with the elemental composition of cement-based cementitious materials. The similar element
847 composition lays a solid foundation for preparing Mn-rich residue-based cementitious materials. However, the
848 presence of harmful components in Mn-rich residue, low activity of raw materials and high-water absorption
849 significantly limit the direct utilization of Mn-rich residue. Therefore, the preparation of Mn-rich residue-based
850 cementitious materials needs to benefit from the excitation of reprocessing technology. As for the application
851 of Mn-rich residue in cementing materials (Wang et al. 2022a), the existing research results show that: 1) As a
852 result of the decomposition of poor crystallinity, calcination can significantly enhance the pozzolanic activity
853 of Mn-rich residue. This is due to the release of calcium oxide as well as the activation of amorphous active
854 aluminium silicates. 2) There is a suitable range of calcination temperature of 800–900 °C in which low
855 temperature limits the dehydration of gypsum and iron phase and then changes the solubility of gypsum
856 followed by Mn-rich residue activity. Moreover, the high-temperature treatment limits the decomposition of
857 heavy metal-containing minerals in Mn-rich residue to form inert and complex oxides such as spinel. 3) The
858 calcination treatment of Mn-rich residue can improve the solidification effect of heavy metal ions.

859 The quasi-sulphoaluminate cementitious materials with the 56-d mechanical properties of 35-65 MPa
860 might also be manufactured utilizing Mn-rich residue, kaolin, and limestone to sinter clinker at 1200 °C, in
861 accordance with the ternary phase diagram of SiO₂-Al₂O₃-CaO (Hou et al. 2012). The quasi-sulfoaluminate
862 cementitious material with 5% gypsum increased its early and long-term strength by about 50% and 30% than
863 that without gypsum, respectively. However, the utilization path is still debatable in terms of the improvement
864 of Mn-rich residue consumption efficiency and the examination of the durability of the product. He et al.
865 (2022a) used Mn-rich residue, barium slag, limestone and bauxite to prepare belite-ye'elimite-alite cement at
866 1350 °C for 1.5 h. The results show that introducing Mn-rich residue can decrease the clinker formation
867 temperature, resulting in cement with 5% gypsum in preparing 28 d compressive strength of 30 MPa. The Mn-
868 rich residue used to fabricate the belite-ye'elimite-ferrite-overfired gypsum cement clinker has excellent
869 mechanical properties. The prepared cement clinker can cure heavy metals (Wang et al. 2023), suggesting the
870 potential realization of high value-added resource reuse of Mn-rich residue. The sintered temperature of this
871 clinker phase is 50~150 °C which is lower than that of traditional sulfoaluminate cement clinker (Wang et al.

872 2023). In addition, the modified Mn-rich residue calcined at 350 °C was used to activate the granulating furnace
873 slag to prepare Mn-rich residue-based slag cement (Wang et al. 2020). Mn-rich residue and modified sulfur
874 can be mixed to produce an acid and alkali-resistant sulfur cement. When the content of sulfur is 45–55%, Mn-
875 rich residue is 20–35%, and the content of sand is 15–30%, the compressive and flexural strength of the cement
876 can reach 48.89–63.17 MPa and 7.12–9.47 MPa, respectively, which are higher than that of ordinary portland
877 cement (Yang et al. 2014). The manufactured sulfur concrete effectively stabilizes the heavy metals in the Mn-
878 rich residue, and the leaching solution is within permissible limits of heavy metals.

879 In a word, calcination provides a new perspective for high value-added resource utilization of Mn-rich
880 residue. The high-temperature treatment of Mn-rich residue to prepare ceramics and clinker reduces the
881 consumption of ore resources and realizes the resource reuse of Mn-rich residue. The prepared Mn-rich
882 residue-based cement clinker makes full use of the oxide of Mn-rich residue, and the presence of heavy metals
883 reduces the calcination temperature, contributing to the carbon emission reduction and carbon peak.

884 4.2 Preparation of Mn-rich residue-based functional materials

885 Mn-rich residue can meet the chemical composition requirements of zeolite preparation (Ma et al. 2023).
886 Using Mn-rich residue as raw material, Li et al. (2015c) prepared the zeolite material at high temperatures
887 using a two-step method with NaOH and NaAlO₂. The zeolite adsorbent with a specific surface area of 35.38
888 m² g⁻¹ was successfully prepared at the Si to Al ratio of 1.5. The maximum adsorption capacities of Ni²⁺ and
889 Mn²⁺ were 128.70 mg g⁻¹ and 66.93 mg g⁻¹, respectively. The synthesized Mn-rich residue-based zeolite can
890 be employed as a promising low-cost adsorbent. Zeolite is often prepared using Mn-rich residue as raw material
891 by microwave alkali fusion activation method heated at 500 °C for 60 min and then crystallized at 100 °C for
892 7 h. The maximum manganese adsorption capacity of the zeolite reached 79.18 mg g⁻¹ (Chang et al. 2019).

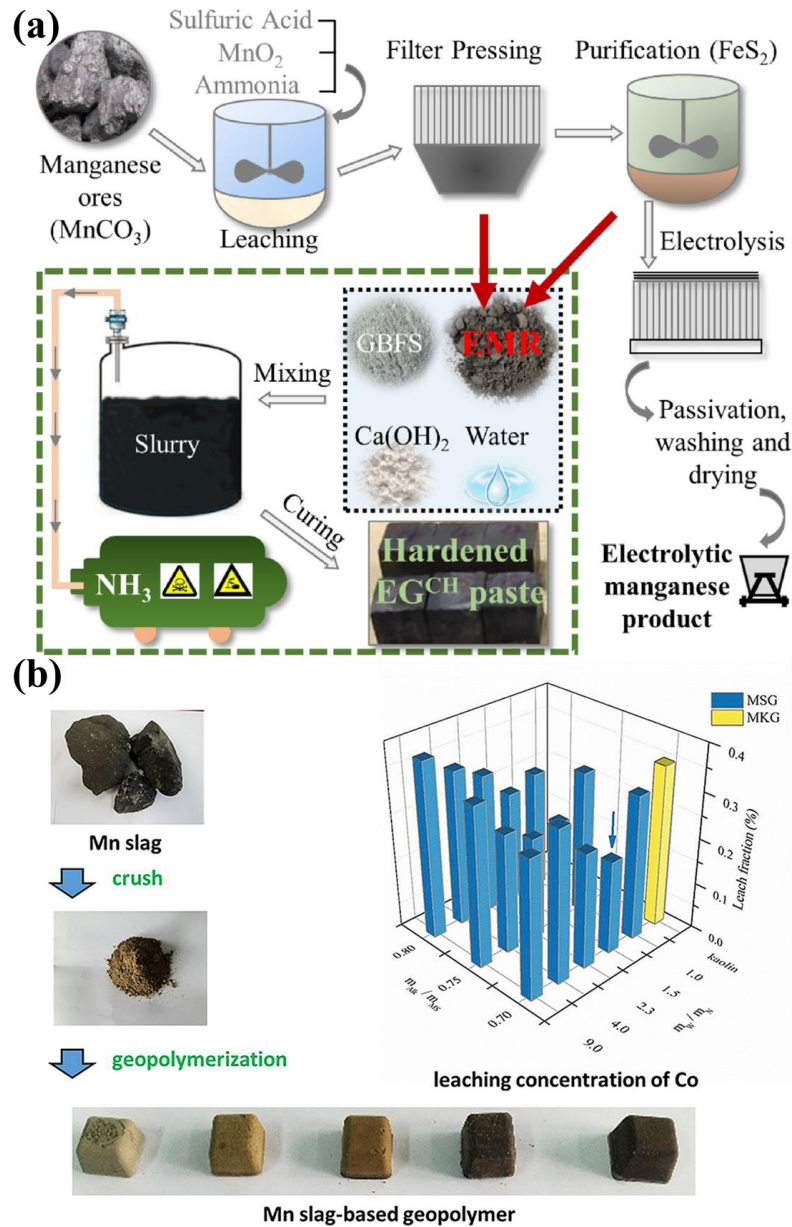
893 Depending on their physicochemical characteristics, Mn-rich residue can be utilized directly as adsorbed
894 materials for treating wastewater with simple or without additional operation. Therefore, Mn-rich residue was
895 effectively employed as a raw material towards the hydrothermal method at 100 °C and pH 12 to manufacture
896 an Mn-rich residue- calcium silicate hydrate (C-S-H) adsorption material with a high specific surface area of
897 205 m² g⁻¹ (Li et al. 2015b). The synthesized adsorbent may effectively adsorb the manganese and phosphoric
898 acid ions in the solution. The Mn-rich residue was added to the Na₂SiO₃ solution and then obtained the
899 suspension by adding MgCl₂ drop-by-drop (Shu et al. 2018b). After a hydrothermal reaction for 24 h, the
900 prepared material with a specific surface area of 500.8 m² g⁻¹ was obtained from the obtained suspension. The
901 adsorption capacity of the synthesized Mn-rich residue-based adsorption material achieved 548.15 mg g⁻¹ after
902 fifty cycles. In addition, Mn-rich residue was put into EDTA-2Na/NaOH solution for ultrasonic etching
903 treatment (Lan et al. 2019a). The nano-sheet structure with 100–200 nm size and a new type of high-activity
904 Fe-Mn oxide nano-composite catalyst was obtained. The prepared material has a high dye removal capacity in
905 a wide pH range of 1~8.5 and a temperature range from 25 to 45 °C, indicating that the process has broad
906 application potential in wastewater treatment. The sieved Mn-rich residue was mixed with the deionized water
907 and oscillated at 13500 rad min⁻¹ for 15 min to form hydrogel (Ma et al. 2020). Thermal activation of Mn-rich
908 residue was achieved by incubating the synthesized hydrogel for 120 min at 800 °C. Pb²⁺ and Cd²⁺ exhibited
909 the highest adsorption capacities of 119.88 mg g⁻¹ and 35.97 mg g⁻¹, respectively. A thermal-activated Mn-rich
910 residue is primarily based on ion exchange, electrostatic attraction, and surface precipitation as its adsorption

911 principle. As a result of electrostatic attraction, the heavy metals in the treated Mn-rich residue are adsorbed
912 on iron-manganese oxides and silicate minerals. Therefore, the Mn-rich residue prepared by thermal activation
913 is an environmentally friendly and effective adsorption material, which can be employed to eliminate heavy
914 metals in the solution.

915 The transitioned metal oxides can also be used as functional materials (Li et al. 2022b). Due to the
916 abundance of manganese and iron phases within Mn-rich residue could be exploited as a raw material or
917 precursor to prepare functional products (Xie et al. 2021b). The Mn-Zn ferrite precursor was prepared by
918 adding the corresponding sulfate and ammonia water according to the proportion of various metal elements.
919 Mn-Zn ferrite was synthesized by burning the precursor at 1200 °C for 5 h while combining it with 0.45%
920 SiO₂ powder. When the doping amount of SiO₂ is 0.45%, the obtained Mn-Zn ferrite has a saturation
921 magnetization of 71.95 emu g⁻¹. Therefore, the preparation of Mn-rich residue-based functional materials helps
922 realize the resource reuse of Mn-rich residue.

923 4.3 Preparation of Mn-rich residue-based soil fertilizer

924 The presence of significant amounts of soluble NH₄⁺-N, sulfate, calcium, iron, and silicon in Mn-rich
925 residue suggested that it may have fertilizer-like positive attributes. The compound fertilizer can be prepared
926 by mixing Mn-rich residue with commercial nitrogen, phosphorus and potassium. The application of mixed
927 fertilizer was more fertile than that of Mn-rich residue alone, which was reflected in the significant increase in
928 grain yield. The Mn-rich residue mixed with inorganic fertilizer significantly enhanced pepper growth
929 compared to fertilization alone. For the preparation of silicomanganese fertilizer containing 6.94% soluble
930 silicon, Mn-rich residue was mixed with CaCO₃, Na₂CO₃ and NaOH and calcined at 400 °C. The mixed
931 Na₂CO₃ with Mn-rich residue increased the active silica content from 0.19 to 12.59% after ball milling
932 activation and calcination (Li et al. 2018a). These results infer that the calcined Mn-rich residue-based material
933 can be employed as silicon fertilizer. In addition, silicate bacteria can be used to activate silica in Mn-rich
934 residue. Since the bioleached solution contained a silicon concentration of 163.27 mg L⁻¹, hence making it a
935 useful source of silicon fertilizer (Lv et al. 2021b).



936

937 Figure 9. Resource utilization results of Mn-rich residue. (a) Mn-rich residue-based cementitious material using
 938 activating blast slag. The labels of GBFS and EMR refer to granulated blast furnace slag and electrolytic manganese
 939 residues, respectively. The mark of EG^{CH} stands for the composite material consisting of GBFS, EMR and calcium
 940 hydroxide. The 28-d hardened samples achieved 30 MPa at 45 wt.% of Mn-rich residue dosage. The Mn²⁺ and NH₄⁺-N
 941 can be well treated by encapsulation and strong alkaline environment. Reprinted with permission of Elsevier from Wang
 942 et al. (2020). (b) Mn-rich residue-based geopolymer by alkali-activation. The MSG and MKG refer to the Mn slag-based
 943 geopolymer and metakaolin-based geopolymer, respectively. The prepared Mn-rich residue geopolymer exhibited a better
 944 nuclear waste immobilization capability. The oxidation environment of the waste material is instrumental in fixation.
 945 Reprinted with permission of Elsevier from Yu et al. (2019).

946 5. High-value resource utilization of Mn-rich residue

947 Mn-rich residue is the main solid waste powder produced in electrolytic manganese and electrolytic
 948 manganese dioxide production. Due to the hydrometallurgical production process, Mn-rich residue contains a

949 lot of sulfates and heavy metals, as well as a lot of quartz, calcium sulfate and aluminosilicate (Duan et al.
950 2011). The existing works on the harmless treatment and resource reuse of Mn-rich residue are mainly based
951 on the chemical composition and mineral properties of Mn-rich residue. As mentioned above, the work in the
952 field of harmless treatment and resource utilization is mainly conducted in the following aspects, including
953 recovery of valuable elements in Mn-rich residue, direct stabilization or solidification and electric restoration
954 of piled Mn-rich residue, resource disposal of building materials, adsorption materials, fertilizers and other
955 functional materials. Implementing these works provides solutions for the hazard-free disposal and resource
956 utilization of Mn-rich residue. However, there are obvious advantages and disadvantages to these approaches.

957 Additionally, due to the complex mineral and chemical compositions of Mn-rich residue, it is more
958 difficult for these resources to be utilized and the breadth of their use. Solid waste is also a misplaced resource
959 that fundamentally attaches the greatest importance to solid waste resources by achieving high-value resource
960 utilization rather than simple consumption and treatment. Although direct and simple disposal can absorb the
961 accumulated reserves of Mn-rich residue, abundant minerals are not exploited and utilized with maximum
962 efficiency, which is also a resource waste to a certain extent. Therefore, by comparing the advantages and
963 disadvantages of various technologies and combining them with the development law of Mn-rich residue, it is
964 worthy of expectation and affirmation to sum up and put forward the efficient, green and high-value resource
965 utilization way of Mn-rich residue.

966 In terms of re-leaching in Mn-rich residue, both water and acid leaching can achieve high-efficiency
967 recovery of Mn^{2+} and NH_4^+-N under the enhanced treatment process. However, water leaching has superior
968 results in handling expenses and environmental safety compared to other techniques since Mn-rich residue
969 would still result in more substantial secondary pollutants and a larger cost of raw materials after acid leaching.
970 Nevertheless, water filtration caused by leaching increases the risk of secondary pollution and disposal costs.
971 The major purpose of the alkaline environment produced by alkaline leaching is to recover silicon. However,
972 acid and base neutralization reactions are generated in the provided alkaline environment, resulting in
973 secondary waste pollution caused by gas overflow. Bioleaching is highly targeted, and the presence of
974 microorganisms will not cause serious secondary pollution. However, bioleaching needs to provide a suitable
975 growth environment for microorganisms to stimulate their reactivity, which increases the burden of economic
976 costs. In addition, severe and unregulated high reactivity limits the widespread use of this technology.

977 The calcination process concentrates and removes Mn^{2+} and NH_4^+-N from Mn-rich residue. On the one
978 hand, the Mn-rich residue can realize the recovery and utilization of sulfur resources after calcination; on the
979 other hand, the thermal activation effect of Mn-rich residue significantly improves the reactivity of Mn-rich
980 residue. It is noteworthy that calcination will increase energy consumption and cause a large amount of
981 greenhouse gas emissions. Direct calcination is widely used to re-extract valuable elements in Mn-rich residue
982 due to energy consumption and gas emission limitations. As it stands now, when economic costs and secondary
983 environmental pollution are considered, the prospect of re-extracting valuable elements from accumulated Mn-
984 rich residue is poor. Compared with the reduction of Mn-rich residue and the resource utilization of Mn-rich
985 residue, the re-extraction of valuable elements of Mn-rich residue should fully consider the coordinated
986 development of economic applicability, environmental friendliness and activity excitation degree.

987 For stabilization or solidification disposal and electric restoration, the technology focuses on harmless

988 disposal of the Mn-rich residue storage site rather than recycling the disposed Mn-rich residue. Therefore, the
989 main application fields of this part of technology are closely related to the soil environment. The stabilization
990 or immobilization of Mn-rich residue mainly reflects that a single chemical (NaOH, CaO or MgO) acts as a
991 curing agent to promote the elimination of Mn^{2+} and NH_4^+-N through an acid-base neutralization reaction. The
992 soluble Mn in Mn-rich residue precipitated and solidified as $Mn(OH)_2$, MnO_2 , and $MnCO_3$, among other
993 insoluble compounds. The treatment mechanism of a single solidified agent is the neutralization reaction
994 between the alkaline environment provided by an alkaline solidified agent and acidic Mn-rich residue to
995 remove Mn^{2+} and NH_4^+-N . Initial Mn-rich residue may require further chemical or physical treatment, resulting
996 in additional disposal costs.

997 Meanwhile, curing Mn-rich residue with chemical reagents increases Mn-rich residue volume. After
998 curing, Mn-rich residue still needs to be treated safely to ensure the long-term stability of the landfill. In
999 addition, the chemical bonding ceramics were formed by acid-base neutralization reaction between magnesium
1000 salts such as MgO, $MgSO_4$, $MgCl_2$ and phosphates such as Na_3PO_4 , Na_2HPO_4 and NaH_2PO_4 to realize harmless
1001 disposal of Mn-rich residue. However, the development of this technology for Mn-rich residue disposal is
1002 limited by the solubility and high economic cost of magnesium materials. As opposed to chemically bonded
1003 ceramics, cement may be able to reduce economic costs to a certain extent. The hydration products formed by
1004 the cement hydration stabilize the soluble salt and heavy metal in the Mn-rich residue via the aluminosilicate
1005 structure, indicating that the effective solidifying of a certain amount of Mn-rich residue can be achieved.
1006 However, the durability and long-term stability of the cured body prepared by acidic Mn-rich residue and
1007 cement are still hidden dangers. Unlike extracting valuable elements, stabilization or solidification can
1008 incorporate other alkaline wastes into the Mn-rich residue disposal system.

1009 Further, the addition of fly ash, furnace slag, steel slag and other solid wastes with potential pozzolanic
1010 properties, phosphate by-products, and other solid wastes for physico-chemical composite curing treatment
1011 can realize harmless disposal of Mn-rich residue and ensure the environmental safety of the storage site. The
1012 synergic solidification or stabilization mechanism of Mn-rich residue and phosphate by-product is mainly
1013 attributed to the interaction of many ions in the two solid wastes to form insoluble substances. Mn-rich residue
1014 co-solidification or stabilization with other wastes significantly decreases costs and enables multi-layer
1015 collaborative treatment of multiple solid wastes. However, the current research results still have pollution risks
1016 due to the lack of long-term durability evaluation systems for cured products. Suppose the solidified cost is
1017 effectively controlled and the durability of the cured product is effectively guaranteed. In that case,
1018 collaborative stabilization or solidification can be employed as a high-efficiency method for the harmless
1019 treatment of Mn-rich residue.

1020 Unlike the solidification or stabilization treatment of Mn-rich residue, electric remediation involves
1021 transferring Mn^{2+} and NH_4^+-N in Mn-rich residue. The migration of unstable soluble ions was changed and
1022 evaluated by adding an electric field enhancer. With the periodic electrolyte replacement, most Mn^{2+} and NH_4^+-
1023 N in Mn-rich residue can be removed. Therefore, electrical repair technology requires a large amount of
1024 electricity to provide continuous electric drive and continuous consumption of electric field enhancers. The
1025 process produces a large amount of waste electrolyte and the secondary pollution caused by the enhancers still
1026 needs further disposal. In short, harmless disposal is imperative. However, the harmless process of Mn-rich

1027 residue is closely related to the economic cost, disposal efficiency and secondary pollution caused by disposal.
1028 Notably, the harmless disposal of Mn-rich residue is the basis of resource utilization. Therefore, the harmless
1029 disposal and resource utilization of Mn-rich residue is intricately linked to building more economical, high
1030 utilization efficient and high-value resource utilization of Mn-rich residue-based materials.

1031 The resource utilization of building materials in Mn-rich residue is because Mn-rich residue contains a
1032 lot of aluminium silicate, hematite, quartz, gypsum, and other potential components which can be used as
1033 construction materials. Cement-based cementitious material, ceramics, roadbed material and brick can be
1034 prepared by Mn-rich residue. It is necessary to monitor the long-term safety risk of the prepared Mn-rich
1035 residue-based material. Currently, the utilization rate of Mn-rich residue in this part is 10~45%. The utilization
1036 efficiency of Mn-rich residue is an important index of the resource disposal of Mn-rich residue, and the
1037 utilization rate of Mn-rich residue-based ceramics can be close to 100%. The prepared Mn-rich residue-based
1038 ceramic can be used as the framework of building materials, providing excellent mechanical properties and
1039 heavy metal solidified effects. However, its main disadvantage is that it requires high-temperature calcination,
1040 which causes energy consumption and greenhouse gas emissions. Hard ceramic frames require more crushing
1041 energy to achieve the target size. In addition, sintering brick can also realize the consumption of a large amount
1042 of Mn-rich residue, but the unbalanced development between energy consumption and the high-value degree
1043 of Mn-rich residue limits the production and use of sintering brick. The development of non-burning bricks
1044 has somewhat improved the above shortcomings because of the rapid reduction of energy consumption.
1045 However, the preparation of Mn-rich residue-based unfired brick often requires the addition of chemicals to
1046 motivate the reactivity of Mn-rich residue and other additives to improve the mechanical properties of the
1047 finished product. Because Mn^{2+} and NH_4^+-N are not treated properly, the prepared Mn-rich residue-based non-
1048 burning bricks have long-term performance and safety risks. For roadbed materials based on Mn-rich residue,
1049 the stable removal of Mn^{2+} and NH_4^+-N and the stability of long-term mechanical properties and toxicity are
1050 prerequisites for its wide application. In addition, the huge demand potential for roadbed materials means a
1051 broad application prospect. Therefore, the harmless disposal of Mn-rich residue has imperative significance.

1052 For Mn-rich residue-based adsorption functional materials, the main target is to translate the
1053 aluminosilicate phase in Mn-rich residue into soluble aluminosilicate under the action of specific activation
1054 and then add aluminate or silicate for secondary treatment to fabricate porous adsorption materials with an
1055 excellent adsorption activity. Therefore, the realization of Mn-rich residue functionalization mainly stimulates
1056 its properties of aluminosilicate, quartz and hematite by physical and chemical methods such as alkaline
1057 additions, hydrothermal method or calcination method to form adsorptive materials such as zeolite. It is of
1058 concern that the secondary waste generated by the prepared adsorbent and its dissolving hazard and durability
1059 still need to be monitored over time for further evaluation. A soil fertilizer developed based on Mn-rich residue
1060 has an improved fertility and growth promotion effect on the growth of specific plants since it contains a large
1061 amount of soluble Mn^{2+} , NH_4^+-N and other micronutrients required for crop growth. However, heavy metal
1062 elements carried by Mn-rich residue migrate into the soil environment with hydraulic power, posing risks to
1063 human health and soil. For the preparation of other functional materials by Mn-rich residue, Mn and Fe
1064 equivalent metals in Mn-rich residue can be developed into infrared radiation or magnetic materials. However,
1065 the use efficiency of Mn-rich residue in preparing such Mn-rich residue-based materials is extremely low,

1066 which means that Mn-rich residue-based functional materials are highly inefficient for eliminating Mn-rich
1067 residue. In addition, secondary pollutants produced during the production process put forward more demanding
1068 requirements for the durability of the final product prepared. Similar to the other materials described above,
1069 the long-time safety and chemical stability of Mn-rich residue-based products must be evaluated and monitored
1070 in long-term tests.

1071 **6. Current deficiencies and further prospects**

1072 The complexity of Mn-rich residue components increases with the hydrometallurgical treatment process
1073 caused by reducing manganese ore grade. Therefore, many soluble sulfates, heavy metals, and components left
1074 over from chemical disposal reagents constitute the main chemical components of Mn-rich residue. The yield
1075 of Mn-rich residue also increases with the decrease in manganese ore grade, which means that the amount of
1076 Mn-rich residue stored in an open pit is difficult to decrease significantly in a short period. Due to this, the
1077 accumulated Mn-rich residue significantly affects the physiological well-being of the public, as well as
1078 polluting and destroying the environment.

1079 From the perspective of soil resources, environmental protection and life health, the harmless treatment
1080 and resource utilization of Mn-rich residue is urgent. It can be seen from the formation process of Mn-rich
1081 residue that the activity of hydrometallurgical Mn-rich residue is lower than that of pyrometallurgical waste.
1082 The presence of inter-layer water, capillary water and chemically bound water further hindered the expansion
1083 of Mn-rich residue activity. Acidic Mn-rich residue affects its application in cement alkaline environments
1084 because it reduces the hydration pH environment of the cementitious materials. There is no way to achieve
1085 efficient, low-cost, and low environmental impact recycling disposal of Mn-rich residue simultaneously by
1086 reducing the harmfulness or recycling.

1087 All the above treatment processes can be divided into heating and non-heating treatment. Specifically,
1088 the physical and chemical disposal of Mn-rich residue without heating mainly aims to recover valuable
1089 elements and cannot achieve good economic benefits, also the formation of potential secondary wastes
1090 deteriorates the environment. Chemical reagents and cementitious materials such as cement were used for
1091 harmless curing treatment of accumulated Mn-rich residue, focusing on the optimal safety control of the Mn-
1092 rich residue storage site. However, this technique requires a large amount of stabilization or solidification agent
1093 consumption, which leads to high disposal costs and low overall disposal efficiency. Moreover, the long-term
1094 durability of solidified products and the long-term environmental impact must be continuously monitored and
1095 evaluated due to the erosion and washing effect of rain during site restoration.

1096 The use of Mn-rich residue as building materials has better progression due to the large demand, which
1097 releases the accumulation pressure of Mn-rich residue to a large extent. The influence of long-term stability
1098 and durability of Mn-rich residue-based building materials is still the biggest obstacle to the resource utilization
1099 of Mn-rich residue building materials. In addition, Mn-rich residue is defined as hazardous solid waste due to
1100 the presence of Mn^{2+} and NH_4^+-N . Therefore, giving full play to the complex components value of Mn-rich
1101 residue, turning waste into treasure and transforming Mn-rich residue into high-value resources are the most
1102 potential disposal solutions for resource utilization in building materials. When Mn-rich residue is prepared
1103 into adsorbent materials, the purpose of waste treatment can be achieved. Mn-rich residue-based adsorption
1104 materials mainly depend on the adsorption potential of SiO_2 . However, the low consumption, secondary

1105 environment and water resources pollution limit its popularization significantly. The same issue occurs when
1106 Mn-rich residue is used to develop soil fertilizers. When Mn-rich residue is used to prepare other functional
1107 materials, its effective utilization rate is low, and secondary solid waste is generated in the production process.
1108 The special characteristics of the low-purity materials that have been manufactured cannot be adequately
1109 guaranteed, and it is necessary to monitor and assess their chemical stability and leaching toxicity over an
1110 extended time.

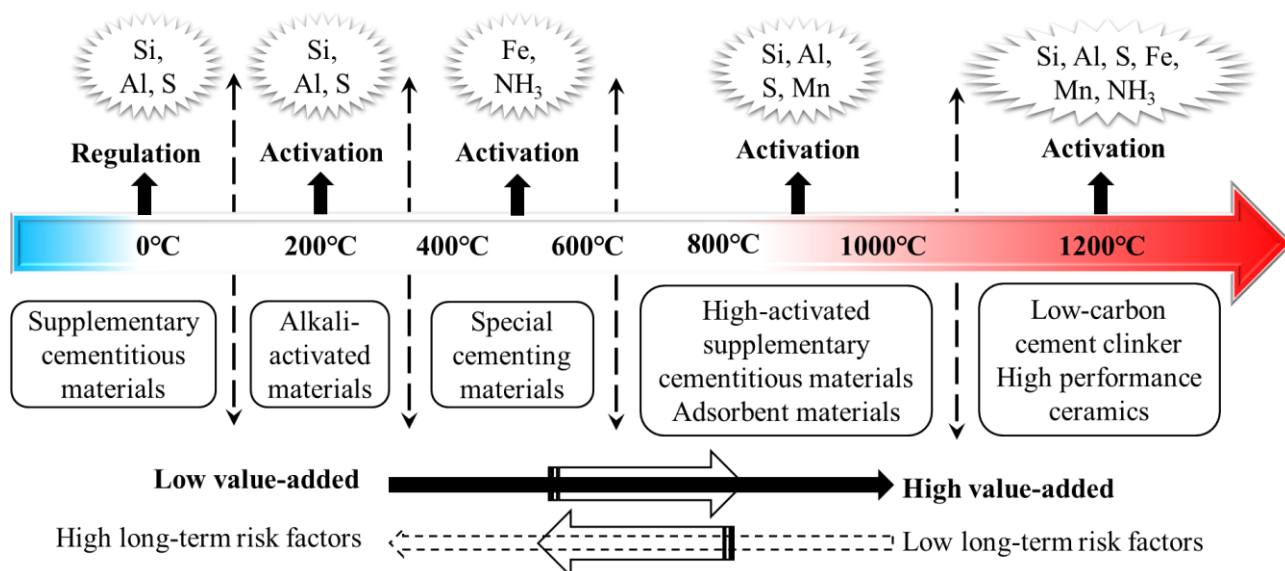
1111 In conclusion, compared with the single absorption treatment, the collaborative disposal of other solid
1112 wastes or building materials stabilized or immobilized by Mn-rich residue has a better prospect of harmless
1113 disposal and resource utilization. As opposed to other consumption types, the use of building materials is an
1114 effective way to maximize Mn-rich residue consumption. The abundant oxides in Mn-rich residue can be used
1115 as effective substitutes for cementitious materials and mineral admixtures in building materials, thus helping
1116 to reduce the consumption of building materials. However, the effective removal of Mn^{2+} and NH_4^+-N from
1117 Mn-rich residue is the prerequisite for resource reuse. In light of the continual consumption of mineral
1118 resources, the exploitation and utilization of solid wastes containing rich mineral resources have a good
1119 prospect. As part of a sustainable development strategy, maximising the utilization of Mn-rich residue
1120 resources and realising their maximum value is imperative. The realization of maximum high-value resource
1121 utilization of Mn-rich residue is due to the synergistic regulation and maximization among disposal efficiency,
1122 harmless degree, environmental disturbance degree and common properties ratio of materials. In other words,
1123 it is necessary to develop and progress toward high disposal efficiency, non-toxicity, no environmental
1124 pollution, high performance, and good long-term stability to maximize the high value-added utilization of Mn-
1125 rich residue in building materials.

1126 All factors coordinate and improve the performance and unit absorption efficiency of Mn-rich residue-
1127 based products to ensure the harmfulness before using Mn-rich residue and the long-term durability of Mn-
1128 rich residue-based products. In this way, the waste can be turned into treasure in a real sense, the disadvantages
1129 of Mn-rich residue can be overcome, the advantages of Mn-rich residue can be highlighted, the misplaced
1130 resources can be reused to the greatest extent, and a high feasibility, high stability and low-cost solution can
1131 be provided for the sustainable development of the building material field with high energy consumption, high
1132 carbon emission and high resource consumption. The high value of Mn-rich residue resource utilization must
1133 fully stimulate the activity advantage of Mn-rich residue mineral components. Currently, the activation
1134 pathways of Mn-rich residue mainly come from physics, chemistry and heat treatment, and relevant research
1135 findings are also shown in the previous studies.

1136 In general, the physical method mainly uses the collision caused by mechanical force to regulate the
1137 particle morphology of Mn-rich residue to change the specific surface area and particle size of Mn-rich residue.
1138 In resource utilization of building materials, finer Mn-rich residue tends to play a more significant role in
1139 micro-powder filling, while Mn-rich residue with larger specific surface areas shows higher activity after the
1140 water absorption characteristics are well treated. In addition, increased work by mechanical forces may lead
1141 to defects in the crystalline mineral lattices of Mn-rich residue, and these defective crystals may exhibit higher
1142 reactivity. The chemical mode is to form new reaction products conducive to resource utilization by introducing
1143 specific chemical substances and chemical reactions with the minerals in Mn-rich residue. The addition of

1144 chemicals can regulate the mineral phase composition of the Mn-rich residue and adjust the water absorption
 1145 characteristics and pH degree of the Mn-rich residue. However, specific and high-purity chemicals often mean
 1146 high disposal costs and the introduction of low-purity chemicals poses a risk of secondary contamination.

1147 At specific temperatures, thermal disposal differs from the previously discussed two treatment methods
 1148 and provides a suitable high-temperature environment where certain Mn-rich residue mineral phases can
 1149 undergo phase transformations (Figure 10). The amorphous mineral phases also significantly improve the
 1150 reactivity of Mn-rich residue. Under high temperatures, Mn-rich residue can cooperate with other solid wastes
 1151 or other chemicals to prepare the clinker phase of cementitious materials. Different Mn-rich residue-based
 1152 cementitious materials can be prepared under specific temperature conditions with different proportions of
 1153 Mn-rich residue and other substances. Mn-rich residue treated at different temperatures must also form high-
 1154 value-added materials according to their component advantages. Therefore, further research should be
 1155 conducted on the evaluation system and the performance safety of sintered Mn-rich residue-based products to
 1156 achieve high value-added utilization and transform waste into wealth.



1157
 1158 Figure 10. The consideration of high value-added resource utilization of Mn-rich residue in thermal treatment. Different
 1159 heat treatment temperatures emphatically change the specific mineral and oxide components of Mn-rich residue. This
 1160 means that different construction materials can be developed for the temperature-modified Mn-rich residue to realize the
 1161 high-value cascade utilization of Mn-rich residue. High energy consumption brought by high temperature can also realize
 1162 the high added value of Mn-rich residue utilization to realize the transformation of waste into wealth. Parameterized
 1163 control of Mn-rich residue at specific temperatures provides a guarantee for high efficiency.

1164 7. Conclusions

1165 The disposal of Mn-rich residue has become an obstacle to the sustainable development of the Mn-rich
 1166 residue industry. Therefore, the source reduction, process safety and high value-added reuse of Mn-rich residue
 1167 have become the most important steps in the disposal of Mn-rich residue. However, the fountainhead reduction
 1168 is limited by the increasing Mn-rich residue production, high-water content, and added chemical agents. For
 1169 harmless disposal of Mn-rich residue, the existing methods are difficult to improve the disposal efficiency,
 1170 meaning the large-scale disposal of Mn-rich residue is difficult to realize. In addition, disposal costs, secondary

1171 contamination, and long-term stability are all barriers that limit their development. Resource utilization is
1172 important for Mn-rich residue, from waste to wealth. The main limitations of Mn-rich residue reuse are
1173 uncertain long-term stability, durability, low value-added, low disposal efficiency and low active utilization.
1174 In addition, the lack of utilization standards, disposal policies and evaluation systems for Mn-rich residue-
1175 based high-value use products severely restricts the pretreatment and reuse of Mn-rich residue. Meanwhile,
1176 the use of Mn-rich residue should not only be the direct disposal of low-activity, low-efficiency and low value-
1177 added; more importantly, the Mn-rich residue resources should be recovered. Several key recommendations
1178 are as follows:

1179 1) The use of chemical additives in the preparation process of electrolytic manganese should be controlled,
1180 such as SO_2 instead of SeO_2 as an antioxidant, rather than artificially increasing the complexity of Mn-rich
1181 residue. Adding a separate sulfide precipitation process enriches and recovers Cu, Ni, Co and other valuable
1182 metals to reduce their entry into Mn-rich residue. Filter or wash the Mn-rich residue before storage or direct
1183 resource utilization, and the washed Mn-rich residue can be directly employed as raw materials of low-value-
1184 added constructed materials.

1185 2) Heat treatment can be used throughout the whole process of reduction, harmless and resource utilization of
1186 Mn-rich residue. Thermal disposal is utilized for ferromanganese enrichment and separation in the Mn-rich
1187 residue reduction, dehydration and NH_4^+ -N removal and Mn^{2+} enrichment in the harmless and activating Mn-
1188 rich residue mineral activity and sintering cementitious materials during resource utilization.

1189 3) Low-temperature calcination can realize the dehydration and conversion of gypsum in Mn-rich residue to
1190 prepare sulfate activator and slag-based cementitious material. The formation of an amorphous phase can
1191 prepare high-activity supplementary cementitious materials and mineral admixtures during high-temperature
1192 calcination. Mn-rich residue can be combined with other solid wastes and minerals to build new cementitious
1193 materials with specific clinker phase proportions by rising the calcination temperature to the sintering interval
1194 of cement clinker.

1195 4) Silicon dioxide in Mn-rich residue is converted to C_2S and C_3S , alumina and sulfate are used for conversion
1196 to calcium sulphoaluminate clinker phases, and the iron phase can be used to prepare ferrite phase solid
1197 solutions such as C_4AF . Other heavy metals, iron and manganese, and sulfur dioxide could be used to construct
1198 a feasible calcining atmosphere, which lowers the sintering temperature and improves the sintering efficiency.
1199 However, the environmental and equipment effects of ammonia and sulfur losses in Mn-rich residue still
1200 require further understanding.

1201 5) The existence forms and release behaviors of Mn^{2+} and NH_4^+ -N in Mn-rich residue under different
1202 conditions need to be monitored and evaluated for a long time. In the process of Mn-rich residue formation,
1203 the source and destination of various chemicals and their effects on soil, ecological environment and human
1204 health need to be deeply scrutinized.

1205 6) Efficient dispersion of Mn-rich residue, reduced moisture content, stabilization or solidification of Mn^{2+} and
1206 NH_4^+ -N, and reactive activation techniques should be strengthened. The evolution behavior of water absorption
1207 and water content of Mn-rich residue in the process of harmless disposal and resource utilization needs to be
1208 quantitatively evaluated.

1209 7) Establish an evaluation system among the process performance, economy and environment of harmless

1210 disposal and resource utilization of Mn-rich residue to standardize the quantitative standard between resource-
1211 based and high-value utilization of Mn-rich residue. The evaluation indexes among carbon emission,
1212 mechanical properties, durability and environmental impact factors were constructed to provide parametric
1213 guidance for the high-value resource utilization of Mn-rich residue.

1214

1215 **Acknowledgements**

1216 The authors thank the Hunan Province Key Field R&D Program (Grant No.2020wk2005), and Central South
1217 University's autonomous Graduate students' Exploration and Innovation Project 2022ZZTS0619 (grant #
1218 506021744).

1219

1220 **Conflict of interest:**

1221 The authors declare no conflict of interest in this paper.

1222

1223 **Ethics approval:**

1224 Not applicable.

1225

1226 **Consent to participate:**

1227 Not applicable.

1228

1229 **Consent for publication:**

1230 Not applicable.

1231

1232 **Availability of data and material:**

1233 Not applicable.

1234

1235 **Code availability:**

1236 Not applicable.

1237

1238 **Author contributions**

1239 Fan Wang, Guangcheng Long, Kunlin Ma, Xiaohui Zeng, Zhuo Tang, Rongzhen Dong, Jionghuang He,
1240 Minghui Shangguan, Qingchun Hu, Rock Keey Liew, Yang Li, John Zhou were involved in writing-review
1241 and editing. Fan Wang and Guangcheng Long were involved in supervision and funding acquisition. Fan Wang,
1242 Guangcheng Long, Qingchun Hu, Rock Keey Liew, Yang Li and John Zhou were involved in figure drawing.
1243 Fan Wang, Guangcheng Long, and John Zhou were involved in conceptualization. Fan Wang and Guangcheng
1244 Long were involved in scope planning.

1245

1246 **References**

1247 Baena-Moreno FM, Leventaki E, Riddell A, Wojtasz-Mucha J, Bernin D (2022). Effluents and residues from

1248 industrial sites for carbon dioxide capture: a review. *Environ Chem Lett*, 1-19. [https://doi.org/10.1007/s10311-](https://doi.org/10.1007/s10311-022-01513-x)
1249 [022-01513-x](https://doi.org/10.1007/s10311-022-01513-x)

1250 Bhoja SK, Tripathy S K, Murthy Y R, Ghosh T K, Kumar C R, Chakraborty D P (2021). Influence of
1251 mineralogy on the dry magnetic separation of ferruginous manganese ore—A comparative study. *Minerals*
1252 11(2), 150. <https://doi.org/10.3390/min11020150>

1253 Chang J, Jia F, Hu C, Ye Q (2019). Adsorption of manganese ion by zeolite synthesized from electrolytic
1254 manganese residue. *Inorg Chem Indust* 51 (9), 61e66. <https://doi.org/10.11962/1006-4990.2019-0239>

1255 Chang J, Srinivasakannan C, Sun X, Jia F (2020) Optimization of microwave-assisted manganese leaching
1256 from electrolyte manganese residue. *Green Process Synth* 9(1), 2-12. <https://doi.org/10.1515/gps-2020-0001>

1257 Chen H, Liu R, Liu Z, Shu J, Tao C (2016). Immobilization of Mn and NH_4^+ -N from electrolytic manganese
1258 residue waste. *Environ Sci Pollut Res* 23, 12352-12361. <https://doi.org/10.1007/s11356-016-6446-2>

1259 Chen H, Long Q, Zhang Y, Qin L (2019). Simultaneous immobilization of NH_4^+ and Mn^{2+} from electrolytic
1260 manganese residue using phosphate and magnesium sources. *RSC Adv* 9(8), 4583-4590.
1261 <https://doi.org/10.1039/C8RA09615E>

1262 Chen H, Long Q, Zhang Y, Wang S, Deng F (2020a). A novel method for the stabilization of soluble
1263 contaminants in electrolytic manganese residue: using low-cost phosphogypsum leachate and
1264 magnesia/calcium oxide. *Ecotox Environ Safe* 194, 110384. <https://doi.org/10.1016/j.ecoenv.2020.110384>

1265 Chen H, Long Q, Zhou F, Shen M (2020b). Elec-accumulating behaviors of manganese in the electrokinetics-
1266 processed electrolytic manganese residue with carbon dioxide and oxalic acid. *J Electroanal Chem* 865, 114162.
1267 <https://doi.org/10.1016/j.jelechem.2020.114162>

1268 Chen J, Li L, Chen G, Peng J, Srinivasakannan C (2017). Rapid thermal decomposition of manganese ore
1269 using microwave heating. *J Alloy Comp* 699, 430-435. <https://doi.org/10.1016/j.jallcom.2016.12.379>

1270 Chen Z, Fang X, Long K, Shen C, Yang Y, Liu J (2021). Using the biocarbonization of reactive magnesia to
1271 cure electrolytic manganese residue. *Geomicrobiol J* 38(8), 709-718.
1272 <https://doi.org/10.1080/01490451.2021.1939812>

1273 Chen Y, Long J, Chen S, Xie Y, Xu Z, Ning Z, Li H (2022). Multi-step purification of electrolytic manganese
1274 residue leachate using hydroxide sedimentation, struvite precipitation, chlorination and coagulation: Advanced
1275 removal of manganese, ammonium, and phosphate. *Sci Total Environ* 805, 150237.
1276 <https://doi.org/10.1016/j.scitotenv.2021.150237>

1277 Cho JH, Eom Y, Lee TG (2014). Stabilization/solidification of mercury-contaminated waste ash using calcium
1278 sodium phosphate (CNP) and magnesium potassium phosphate (MKP) processes. *J Hazard Mater* 278, 474-
1279 482. <https://doi.org/10.1016/j.jhazmat.2014.06.026>

1280 China Mineral Resources 2021. Ministry of Natural Resources, PRC. GEOLOGICAL PUBLISHING HOUSE.
1281 BEIJING. https://www.mnr.gov.cn/dt/ywbb/202110/t20211022_2699855.html

1282 Ding F, Zhan J, Wang Z, Chai L, Zhang C (2016). Simultaneous leaching of low grade bismuthinite and
1283 pyrolusite ores in hydrochloric acid medium. *Hydrometallurgy* 166, 279-284.
1284 <https://doi.org/10.1016/j.hydromet.2016.08.009>

1285 Deng Y, Shu J, Lei T, Zeng X, Li B, Chen M (2021). A green method for Mn^{2+} and NH_4^+ -N removal in
1286 electrolytic manganese residue leachate by electric field and phosphorus ore flotation tailings. *Separ Purif*

1287 Technol 270, 118820. <https://doi.org/10.1016/j.seppur.2021.118820>

1288 Du B, Zhou C, Dan Z, Luan Z, Duan N (2014a). Preparation and characteristics of steam-autoclaved bricks
1289 produced from electrolytic manganese solid waste. *Constr Build Mater* 50, 291-299.
1290 <https://doi.org/10.1016/j.conbuildmat.2013.09.055>

1291 Du B, Zhou CB, Duan N (2014b). Recycling of electrolytic manganese solid waste in autoclaved bricks
1292 preparation in China. *J Mater Cycles Waste Manage* 16, 258-269. <https://doi.org/10.1007/s10163-013-0181-2>

1293 Du B, Hou D, Duan N, Zhou C, Wang J, Dan Z (2015). Immobilization of high concentrations of soluble Mn
1294 (II) from electrolytic manganese solid waste using inorganic chemicals. *Environ Sci Pollut Res* 22, 7782-7793.
1295 <https://doi.org/10.1007/s11356-015-4197-0>

1296 Duan J, Feng S, He W, Li R, Zhang P, Zhang Y (2021). TG-FTIR and Py-GC/MS combined with kinetic model
1297 to study the pyrolysis characteristics of electrolytic manganese residue. *J Anal and Appl Pyrol* 159, 105203.
1298 <https://doi.org/10.1016/j.jaap.2021.105203>

1299 Duan N, Fan W, Changbo Z, Chunlei Z, Hongbing Y (2010). Analysis of pollution materials generated from
1300 electrolytic manganese industries in China. *Resour Conserv Recy* 54(8), 506-511.
1301 <https://doi.org/10.1016/j.resconrec.2009.10.007>

1302 Duan N, Zhou C, Chen B, Jiang W, Xin B (2011). Bioleaching of Mn from manganese residues by the mixed
1303 culture of *Acidithiobacillus* and mechanism. *J Chem Technol Biotechnol* 86, 832e837.
1304 <https://doi.org/10.1002/jctb.2596>.

1305 Elliott R, Barati M (2020). A review of the beneficiation of low-grade manganese ores by magnetic separation.
1306 *Can Metall Quart* 59(1), 1-16. <https://doi.org/10.1080/00084433.2020.1711654>

1307 He D, Shu J, Wang R, Chen M, Wang R, Gao Y, Wang N (2021a). A critical review on approaches for
1308 electrolytic manganese residue treatment and disposal technology: Reduction, pretreatment, and reuse. *J*
1309 *Hazard Mater* 418, 126235. <https://doi.org/10.1016/j.jhazmat.2021.126235>

1310 He D, Luo Z, Zeng X, Chen Q, Zhao Z, Cao W, Chen M (2022a). Electrolytic manganese residue disposal
1311 based on basic burning raw material: Heavy metals solidification/stabilization and long-term stability. *Sci Total*
1312 *Environ* 825, 153774. <https://doi.org/10.1016/j.scitotenv.2022.153774>

1313 He S, Jiang D, Hong M, Liu Z (2021b). Hazard-free treatment and resource utilisation of electrolytic
1314 manganese residue: A review. *J Clean Prod* 306, 127224. <https://doi.org/10.1016/j.jclepro.2021.127224>

1315 He S, Wilson BP, Lundström M, Liu Z (2021c). Hazard-free treatment of electrolytic manganese residue and
1316 recovery of manganese using low temperature roasting-water washing process. *J Hazard Mater* 402, 123561.
1317 <https://doi.org/10.1016/j.jhazmat.2020.123561>

1318 He W, Li R, Zhang Y, Nie D (2022b). Synergistic use of electrolytic manganese residue and barium slag to
1319 prepare belite-sulphoaluminate cement study. *Constr. Build. Mater.* 326, 126672.
1320 <https://doi.org/10.1016/j.conbuildmat.2022.126672>

1321 Ho HJ, Iizuka A, Lee CH, Chen WS (2022). Mineral carbonation using alkaline waste and byproducts to reduce
1322 CO₂ emissions in Taiwan. *Environ Chem Lett*, 1-20. <https://doi.org/10.1007/s10311-022-01518-6>

1323 Hossain MR, Sultana R, Patwary MM, Khunga N, Sharma P, Shaker SJ (2022). Self-healing concrete for
1324 sustainable buildings. A review. *Environ Chem Lett*, 1-9. <https://doi.org/10.1007/s10311-021-01375-9>

1325 Hou P, Qian J, Wang Z, Deng C (2012). Production of quasi-sulphoaluminate cementitious materials with

1326 electrolytic manganese residue. *Cement Concr Comp* 34, 248e254.
1327 <https://doi.org/10.1016/j.cemconcomp.2011.10.003>.

1328 Huang Y, Zhang Q (2022). Highly efficient removal of Cu (II) with modified electrolytic manganese residue
1329 as a novel adsorbent. *Arab J Sci Eng* 47(5), 6577-6589. <https://doi.org/10.1007/s13369-021-06506-6>

1330 Huang Q, Cai X, Chen M, Yang Q, Fan S, Zhang Y, Huang Z (2022). A stepwise processing strategy for treating
1331 manganese residue and the remediation of hexavalent chromium in water and soil by manganese residue-
1332 derived (Fe, Mn)C₂O₄. *Chem Eng J* 436, 135258. <https://doi.org/10.1016/j.cej.2022.135258>

1333 Jiang L (2020). Heat treatment parameters of preparing glass-ceramic with electrolytic manganese residue and
1334 their properties. *J Therm Anal Calorim* 140, 1737e1744. <https://doi.org/10.1007/s10973-019-08935-w>.

1335 Kim H T, Lee T G (2017). A simultaneous stabilization and solidification of the top five most toxic heavy
1336 metals (Hg, Pb, As, Cr, and Cd). *Chemosphere* 178, 479-485.
1337 <https://doi.org/10.1016/j.chemosphere.2017.03.092>

1338 Lan J, Sun Y, Guo L, Du Y, Du D, Zhang T C, Ye H (2019a). Highly efficient removal of As (V) with modified
1339 electrolytic manganese residues (M-EMRs) as a novel adsorbent. *J Alloy Comp* 811, 151973.
1340 <https://doi.org/10.1016/j.jallcom.2019.151973>

1341 Lan J, Sun Y, Guo L, Li Z, Du D, Zhang TC (2019b). A novel method to recover ammonia, manganese and
1342 sulfate from electrolytic manganese residues by bio-leaching. *J Clean Prod* 223, 499e507.
1343 <https://doi.org/10.1016/j.jclepro.2019.03.098>.

1344 Lan J, Sun Y, Tian H, Zhan W, Du Y, Ye H, Hou H (2021a). Electrolytic manganese residue-based cement for
1345 manganese ore pit backfilling: Performance and mechanism. *J Hazard Mater* 411, 124941.
1346 <https://doi.org/10.1016/j.jhazmat.2020.124941>

1347 Lan J, Dong Y, Xiang Y, Zhang S, Mei T, Hou H. (2021b). Selective recovery of manganese from electrolytic
1348 manganese residue by using water as extractant under mechanochemical ball grinding: Mechanism and
1349 kinetics. *J Hazard Mater* 415, 125556. <https://doi.org/10.1016/j.jhazmat.2021.125556>

1350 Lan J, Sun Y, Chen X, Zhan W, Du Y, Zhang TC, Hou H (2021c). Bio-leaching of manganese from electrolytic
1351 manganese slag by *Microbacterium trichothecenolyticum* Y1: Mechanism and characteristics of microbial
1352 metabolites. *Bioresour Technol* 319, 124056. <https://doi.org/10.1016/j.biortech.2020.124056>

1353 Li C, Zhong H, Wang S, Xue J, Zhang Z (2015a). Removal of basic dye (methylene blue) from aqueous
1354 solution using zeolite synthesized from electrolytic manganese residue. *J Ind Eng Chem* 23, 344-352.
1355 <https://doi.org/10.1016/j.jiec.2014.08.038>

1356 Li C, Zhang Q (2020). Preparation and property of unfired brick using electrolytic manganese residue. In
1357 *Journal of Physics: Conference Series* (Vol. 1681, No. 1, p. 012009). IOP Publishing.
1358 <https://doi.org/10.1088/1742-6596/1681/1/012009>

1359 Li CX, Zhong H, Shuai W, Xue JR, Wu FF, Zhang ZY (2015b). Manganese extraction by reduction–acid
1360 leaching from low-grade manganese oxide ores using CaS as reductant. *T Nonferr Metal Soc* 25(5), 1677-1684.
1361 [https://doi.org/10.1016/S1003-6326\(15\)63772-4](https://doi.org/10.1016/S1003-6326(15)63772-4)

1362 Li C, Zhong H, Wang S, Xue J, Zhang Z (2015c). A novel conversion process for waste residue: Synthesis of
1363 zeolite from electrolytic manganese residue and its application to the removal of heavy metals. *Colloid Surface*
1364 *A* 470, 258-267. <https://doi.org/10.1016/j.colsurfa.2015.02.003>

1365 Li Q, Liu Q, Peng B, Chai L, Liu H (2016). Self-cleaning performance of TiO₂-coating cement materials
1366 prepared based on solidification/stabilization of electrolytic manganese residue. *Constr Build Mater* 106, 236-
1367 242. <https://doi.org/10.1016/j.conbuildmat.2015.12.088>

1368 Li J, Du D, Peng Q, Wu C, Lv K, Ye H, Zhan W (2018a). Activation of silicon in the electrolytic manganese
1369 residue by mechanical grinding-roasting. *J Clean Prod* 192, 347-353.
1370 <https://doi.org/10.1016/j.jclepro.2018.04.184>

1371 Li J, Sun P, Li J, Lv Y, Ye H, Shao L, Du D (2020a). Synthesis of electrolytic manganese residue-fly ash based
1372 geopolymers with high compressive strength. *Constr Build Mater* 248, 118489.
1373 <https://doi.org/10.1016/j.conbuildmat.2020.118489>

1374 Li J, Lv Y, Jiao X, Sun P, Li J, Wuri L, Zhang T C (2020b). Electrolytic manganese residue based autoclaved
1375 bricks with Ca(OH)₂ and thermal-mechanical activated K-feldspar additions. *Constr Build Mater* 230, 116848.
1376 <https://doi.org/10.1016/j.conbuildmat.2019.116848>

1377 Li X, Zeng Y, Chen F, Wang T, Li Y, Chen Y, Zhou M (2018b). Synthesis of zeolite from carbothermal reduction
1378 electrolytic manganese residue for the removal of macrolide antibiotics from aqueous solution. *Materials*
1379 11(11), 2133. <https://doi.org/10.3390/ma11112133>

1380 Li X, Zhou M, Chen F, Li J, Li Y, Wang Y, Hou H (2021). Clean stepwise extraction of valuable components
1381 from electrolytic manganese residue via reducing leaching-roasting. *ACS Sustainable Chem Eng* 9(24), 8069-
1382 8079. <https://doi.org/10.1021/acssuschemeng.0c09286>

1383 Li B, Shu J, Wu Y, Su P, Yang Y, Chen M, Liu Z (2022a). Enhanced removal of Mn²⁺ and NH₄⁺-N in electrolytic
1384 manganese residue leachate by electrochemical and modified phosphate ore flotation tailings. *Separ Purif*
1385 *Technol* 291, 120959. <https://doi.org/10.1016/j.seppur.2022.120959>

1386 Li M, He Z, Zhong H, Sun W, Hu L, Luo M (2022b). (Fe_{0.67}Mn_{0.33})OOH riched in oxygen vacancies facilitated
1387 the PMS activation of modified EMR for refractory foaming agent removal from mineral processing
1388 wastewater. *Chem Eng J* 441, 136024. <https://doi.org/10.1016/j.cej.2022.136024>

1389 Liu B, Zhang Y, Lu M, Su Z, Li G, Jiang T (2019). Extraction and separation of manganese and iron from
1390 ferruginous manganese ores: A review. *Miner Eng* 131, 286-303. <https://doi.org/10.1016/j.mineng.2018.11.016>

1391 Liu Y, Lin Q, Li L, Fu J, Zhu Z, Wang C, Qian D (2014). Study on hydrometallurgical process and kinetics of
1392 manganese extraction from low-grade manganese carbonate ores. *Int J Mining Sci Techno* 24(4), 567-571.
1393 <https://doi.org/10.1016/j.ijmst.2014.05.022>

1394 Lv Y, Li J, Ye H, Du D, Li J, Sun P, Ma M, Wen J (2019). Bioleaching behaviors of silicon and metals in
1395 electrolytic manganese residue using silicate bacteria. *J Clean Prod* 228, 901e909.
1396 <https://doi.org/10.1016/j.jclepro.2019.04.289>.

1397 Lv Y, Li J, Liu X, Chen B, Zhang M, Chen Z, Zhang TC (2021a). Screening of silicon-activating bacteria and
1398 the activation mechanism of silicon in electrolytic manganese residue. *Environ Res* 202, 111659.
1399 <https://doi.org/10.1016/j.envres.2021.111659>

1400 Lv Y, Li J, Chen Z, Ye H, Du D, Shao L, Ma M (2021b). Species identification and mutation breeding of
1401 silicon-activating bacteria isolated from electrolytic manganese residue. *Environ Sci Pollut Res* 28, 1491-1501.
1402 <https://doi.org/10.1007/s11356-020-10526-4>

1403 Ma M, Du Y, Bao S, Li J, Wei H, Lv Y, Song X, Zhang T, Du D (2020). Removal of cadmium and lead from

1404 aqueous solutions by thermal activated electrolytic manganese residues. *Sci Total Environ* 748, 141490.
1405 <https://doi.org/10.1016/j.scitotenv.2020.141490>.

1406 Ma M, Wang T, Ke X, Liu Y, Song Y, Shang X, Han Q (2023). A novel slag composite for the adsorption of
1407 heavy metals: Preparation, characterization and mechanisms. *Environ Res* 216, 114442.
1408 <https://doi.org/10.1016/j.envres.2022.114442>

1409 Mpho M, Samson B, Ayo A (2013). Evaluation of reduction roasting and magnetic separation for upgrading
1410 Mn/Fe ratio of fine ferromanganese. *Int J Min Sci Techno* 23(4), 537-541.
1411 <https://doi.org/10.1016/j.ijmst.2013.07.012>

1412 Muriana R A. (2015). Responses of Ka'oje metallurgical manganese ore to gravity concentration techniques.
1413 *Inter J Scient Eng Technol* 4(7), 392-396. <https://doi.org/10.17950/ijset/v4s7/702>

1414 Nandhini R, Berslin D, Sivaprakash B, Rajamohan N, Vo DVN (2022). Thermochemical conversion of
1415 municipal solid waste into energy and hydrogen: a review. *Environ Chem Lett*, 20(3), 1645-1669.
1416 <https://doi.org/10.1007/s10311-022-01410-3>

1417 Ouhadi VR, Yong RN, Deiranlou M (2021). Enhancement of cement-based solidification/stabilization of a
1418 lead-contaminated smectite clay. *J Hazard Mater* 403, 123969. <https://doi.org/10.1016/j.jhazmat.2020.123969>

1419 Oyelola A O (2020). Upgrading a low grade Wasagu–Danko (Nigeria) manganese ore using gravity separation
1420 methods. *Indian J Eng* 17(48), 357-362.
1421 http://www.discoveryjournals.org/engineering/current_issue/2020/v17/n48/A5.pdf

1422 Peng T, Xu L, Chen H (2010). Preparation and characterization of high specific surface area Mn₃O₄ from
1423 electrolytic manganese residue. *Cent Eur J Chem* 8(5), 1059e1068. [https://doi.org/10.2478/s11532-010-0081-](https://doi.org/10.2478/s11532-010-0081-4)
1424 [4](https://doi.org/10.2478/s11532-010-0081-4).

1425 Priyadarshi R, Khan A, Ezati P, Tammina SK, Priyadarshi S, Bhattacharya T, Rhim JW (2023). Sulfur recycling
1426 into value-added materials: a review. *Environ Chem Lett*, 1-27. <https://doi.org/10.1007/s10311-023-01575-5>

1427 Qian J, Hou P, Wang Z, Qu Y (2012). Crystallization characteristic of glass-ceramic made from electrolytic
1428 manganese residue. *J Wuhan Univ Technol Mater Sci. Ed. 2*, 45e49. [https://doi.org/10.1007/s11595-012-0404-](https://doi.org/10.1007/s11595-012-0404-8)
1429 [8](https://doi.org/10.1007/s11595-012-0404-8).

1430 Qiao D, Qian J, Wang Q, Dang Y, Zhang H, Zeng D (2010). Utilization of sulfate-rich solid wastes in rural
1431 road construction in the Three Gorges Reservoir. *Resour Conserv Recyc* 54(12), 1368-1376.
1432 <https://doi.org/10.1016/j.resconrec.2010.05.013>

1433 Rodrigues FA, Joekes I (2011). Cement industry: sustainability, challenges and perspectives. *Environ Chem*
1434 *Lett*, 9, 151-166. <https://doi.org/10.1007/s10311-010-0302-2>

1435 Shu J, Liu R, Liu Z, Chen H, Tao C (2016). Enhanced extraction of manganese from electrolytic manganese
1436 residue by electrochemical. *J Electroanal Chem* 780, 32-37. <https://doi.org/10.1016/j.jelechem.2016.08.033>

1437 Salami BA, Oyehan TA, Tanimu A, Olabintan AB, Ibrahim M, Sanni-Anibire MO, Saleh TA (2022). Cement-
1438 based batteries design and performance. A review. *Environ Chem Lett* 20, 1671–1694.
1439 <https://doi.org/10.1007/s10311-022-01389-x>

1440 Shu J, Liu R, Liu Z, Chen H, Tao C (2017). Leaching of manganese from electrolytic manganese residue by
1441 electro-reduction. *Environ Technol* 38(16), 2077-2084. <https://doi.org/10.1080/09593330.2016.1245789>

1442 Shu J, Wu H, Liu R, Liu Z, Li B, Chen M, Tao C (2018a). Simultaneous stabilization/solidification of Mn²⁺

1443 and NH_4^+ -N from electrolytic manganese residue using MgO and different phosphate resource. *Ecotox Environ*
1444 *Safe* 148, 220-227. <https://doi.org/10.1016/j.ecoenv.2017.10.027>

1445 Shu J, Liu R, Wu H, Liu Z, Sun X, Tao C (2018b). Adsorption of methylene blue on modified electrolytic
1446 manganese residue: kinetics, isotherm, thermodynamics and mechanism analysis. *J Taiwan Inst Chem E* 82,
1447 351–359. <https://doi.org/10.1016/j.jtice.2017.11.020>

1448 Shu J, Chen M, Wu H, Li B, Wang B, Li B, Liu Z (2019a). An innovative method for synergistic
1449 stabilization/solidification of Mn^{2+} , NH_4^+ -N, PO_4^{3-} and F^- in electrolytic manganese residue and
1450 phosphogypsum. *J Hazard Mater* 376, 212-222. <https://doi.org/10.1016/j.jhazmat.2019.05.017>

1451 Shu J, Wu H, Chen M, Peng H, Li B, Liu R, Hu Z (2019b). Fractional removal of manganese and ammonia
1452 nitrogen from electrolytic metal manganese residue leachate using carbonate and struvite precipitation. *Water*
1453 *Res* 153, 229-238. <https://doi.org/10.1016/j.watres.2018.12.044>

1454 Shu J, Sun X, Liu R, Liu Z, Wu H, Chen M, Li B (2019c). Enhanced electrokinetic remediation of manganese
1455 and ammonia nitrogen from electrolytic manganese residue using pulsed electric field in different enhancement
1456 agents. *Ecotox Environ Saf* 171, 523e529. <https://doi.org/10.1016/j.ecoenv.2019.01.025>.

1457 Shu J, Lin F, Chen M, Li B, Wei L, Wang J, Wang R (2020a). An innovative method to enhance manganese
1458 and ammonia nitrogen leaching from electrolytic manganese residue by surfactant and anode iron plate.
1459 *Hydrometallurgy* 193, 105311. <https://doi.org/10.1016/j.hydromet.2020.105311>

1460 Shu J, Cai L, Zhao J, Feng H, Chen M, Zhang X, Liu R (2020b). A low cost of phosphate-based binder for
1461 Mn^{2+} and NH_4^+ -N simultaneous stabilization in electrolytic manganese residue. *Ecotox Environ Safe* 205,
1462 111317. <https://doi.org/10.1016/j.ecoenv.2020.111317>

1463 Shu J, Wu Y, Deng Y, Lei T, Huang J, Han Y, Chen M (2021). Enhanced removal of Mn^{2+} and NH_4^+ -N in
1464 electrolytic manganese metal residue using washing and electrolytic oxidation. *Sep Purif Technol* 270,
1465 118798. <https://doi.org/10.1016/j.seppur.2021.118798>

1466 Silva MA, Testolin RC, Godinho-Castro AP, Corrêa AX, Radetski CM (2011). Environmental impact of
1467 industrial sludge stabilization/solidification products: chemical or ecotoxicological hazard evaluation? *J*
1468 *Hazard Mater* 192(3), 1108-1113. <https://doi.org/10.1016/j.jhazmat.2011.06.019>

1469 Singh V, Ghosh T K, Ramamurthy Y, Tathavadkar V (2011). Beneficiation and agglomeration process to utilize
1470 low-grade ferruginous manganese ore fines. *Int J Miner Process* 99(1-4), 84-86.
1471 <https://doi.org/10.1016/j.minpro.2011.03.003>

1472 Singh V, Chakraborty T, Tripathy S K (2020). A review of low grade manganese ore upgradation processes.
1473 *Miner Process Extr Met Rev* 41(6), 417-438. <https://doi.org/10.1080/08827508.2019.1634567>

1474 Sorensen B, Gaal S, Ringdalen E, Tangstad M, Kononov R, Ostrovski O (2010). Phase compositions of
1475 manganese ores and their change in the process of calcination. *Int J Miner Process* 94(3-4), 101-110.
1476 <https://doi.org/10.1016/j.minpro.2010.01.001>

1477 Sun WY, Su SJ, Wang QY, Ding SL (2013). Lab-scale circulation process of electrolytic manganese production
1478 with low-grade pyrolusite leaching by SO_2 . *Hydrometallurgy* 133, 118-125.
1479 <https://doi.org/10.1016/j.hydromet.2012.12.005>

1480 Tang B, Gao S, Wang Y, Liu X, Zhang N 2019. Pore structure analysis of electrolytic manganese residue based
1481 permeable brick by using industrial CT. *Constr Build Mater* 208, 697-709.

1482 <https://doi.org/10.1016/j.conbuildmat.2019.03.066>

1483 Tian Y, Shu J, Chen M, Wang J, Wang Y, Luo Z, Wang R, Yang F, Xiu F, Sun Z (2019). Manganese and
1484 ammonia nitrogen recovery from electrolytic manganese residue by electric field enhanced leaching. *J Clean*
1485 *Prod* 236, 117708. <https://doi.org/10.1016/j.jclepro.2019.117708>

1486 Tripathy S K, Banerjee P K, Suresh N (2015). Effect of desliming on the magnetic separation of low-grade
1487 ferruginous manganese ore. *Int J Min Met Mater* 22, 661-673. <https://doi.org/10.1007/s12613-015-1120-0>

1488 USGS 2022. Mineral Commodity Summaries by National Minerals Information Center.
1489 <https://www.usgs.gov/centers/national-minerals-information-center/mineral-commodity-summaries>

1490 Velusamy K, Periyasamy S, Kumar PS, Vo DVN, Sindhu J, Sneka D, Subhashini B (2021). Advanced
1491 techniques to remove phosphates and nitrates from waters: a review. *Environ Chem Lett*, 19, 3165-3180.
1492 <https://doi.org/10.1007/s10311-021-01239-2>

1493 Wang D, Wang Q, Xue J (2020). Reuse of hazardous electrolytic manganese residue: Detailed leaching
1494 characterization and novel application as a cementitious material. *Resour Conserv Recy* 154, 104645.
1495 <https://doi.org/10.1016/j.resconrec.2019.104645>

1496 Wang F, Long G, Bai M, Wang J, Zhou J L, Zhou X (2022a). Application of electrolytic manganese residues
1497 in cement products through pozzolanic activity motivation and calcination. *J Clean Prod* 338, 130629.
1498 <https://doi.org/10.1016/j.jclepro.2022.130629>

1499 Wang F, Long G, Bai M, Wang J, Yang Z, Zhou X, Zhou J L (2022b). Cleaner and safer disposal of electrolytic
1500 manganese residues in cement-based materials using direct electric curing. *J Clean Prod* 356, 131842.
1501 <https://doi.org/10.1016/j.jclepro.2022.131842>

1502 Wang F, Long G, Bai M, Wang J, Shi Y, Zhou X, Zhou JL (2023). A new perspective on Belite-ye'elimited-
1503 ferrite cement manufactured from electrolytic manganese residue: Production, properties, and environmental
1504 analysis. *Cement Concrete Res* 163, 107019. <https://doi.org/10.1016/j.cemconres.2022.107019>

1505 Wang J, Peng B, Chai L, Zhang Q, Liu Q (2013). Preparation of electrolytic manganese residue-ground
1506 granulated blast furnace slag cement. *Powder technol* 241, 12-18.
1507 <https://doi.org/10.1016/j.powtec.2013.03.003>

1508 Wang N, Fang Z, Peng S, Cheng D, Du B, Zhou C (2016). Recovery of soluble manganese from electrolyte
1509 manganese residue using a combination of ammonia and CO₂. *Hydrometallurgy* 164, 288-294.
1510 <https://doi.org/10.1016/j.hydromet.2016.06.019>

1511 Wang Y, Gao S, Liu X, Tang B, Mukiza E, Zhang N (2019). Preparation of non-sintered permeable bricks
1512 using electrolytic manganese residue: Environmental and NH₃-N recovery benefits. *J Hazard Mater* 378,
1513 120768. <https://doi.org/10.1016/j.jhazmat.2019.120768>

1514 Wang Y, Zhang N, Ren Y, Xu Y, Liu X (2021). Effect of electrolytic manganese residue in fly ash-based
1515 cementitious material: Hydration behavior and microstructure. *Materials* 14(22), 7047.
1516 <https://doi.org/10.3390/ma14227047>

1517 Wu Y, Shi B, Ge W, Yan C J, Yang X (2015). Magnetic separation and magnetic properties of low-grade
1518 manganese carbonate ore. *JOM* 67, 361-368. <https://doi.org/10.1007/s11837-014-1212-8>

1519 Wu FF, Li XP, Zhong H, Wang S (2016). Utilization of electrolytic manganese residues in production of porous
1520 ceramics. *Int J Appl Ceram Technol* 13(3), 511-521. <https://doi.org/10.1111/ijac.12502>

1521 Wu JF, Song MS, Xu XH, Rao ZG, Cheng H (2013). Analysis of the sintering properties of electrolytic
1522 manganese residue. *Adv Mater Res* 785, 1055–1059. [https://doi.org/10.4028/www.scientific.net/AMR.785-](https://doi.org/10.4028/www.scientific.net/AMR.785-786.1055)
1523 [786.1055](https://doi.org/10.4028/www.scientific.net/AMR.785-786.1055)

1524 Xie H, Li S, Guo Z, Xu Z (2021a). Extraction of lead from electrolytic manganese anode mud by microwave
1525 coupled ultrasound technology. *J Hazard Mater* 407, 124622. <https://doi.org/10.1016/j.jhazmat.2020.124622>

1526 Xie F, Liu H, Bai M, Wen S, Xu F, Zhao J, Liu W (2021b). Flexible LiZnTiMn ferrite/ PDMS composites with
1527 enhanced magnetic-dielectric properties for miniaturized application. *Ceram Int* 47, 1121e1125.
1528 <https://doi.org/10.1016/j.ceramint.2020.08.228>

1529 Xin B, Li T, Li X, Dan Z, Xu F, Duan N, Zhang H (2015). Reductive dissolution of manganese from manganese
1530 dioxide ore by autotrophic mixed culture under aerobic conditions. *J Clean Prod* 92, 54-64.
1531 <https://doi.org/10.1016/j.jclepro.2014.12.060>

1532 Xiong S, Li X, Liu P, Hao S, Hao F, Yin Z, Liu J (2018). Recovery of manganese from low-grade pyrolusite
1533 ore by reductively acid leaching process using lignin as a low cost reductant. *Miner Eng* 125, 126-132.
1534 <https://doi.org/10.1016/j.mineng.2018.06.003>

1535 Xu Y, Liu X, Zhang Y, Tang B, Mukiza E (2019). Investigation on sulfate activation of electrolytic manganese
1536 residue on early activity of blast furnace slag in cement-based cementitious material. *Constr Build Mater* 229,
1537 116831. <https://doi.org/10.1016/j.conbuildmat.2019.116831>

1538 Xue F, Wang T, Zhou M, Hou H (2020). Self-solidification/stabilisation of electrolytic manganese residue:
1539 Mechanistic insights. *Constr Build Mater* 255, 118971. <https://doi.org/10.1016/j.conbuildmat.2020.118971>

1540 Yang C, Lv X, Tian X, Wang Y, Komarneni S (2014). An investigation on the use of electrolytic manganese
1541 residue as filler in sulfur concrete. *Construct Build Mater* 73, 305e310.
1542 <https://doi.org/10.1016/j.conbuildmat.2014.09.046>.

1543 Yang Y, Shu J, Zhang L, Su P, Meng W, Wan Q, Ming X (2021). Enhanced Leaching of Mn from Electrolytic
1544 Manganese Anode Slime via an Electric Field. *Energy Fuels* 35(24), 20224-20230.
1545 <https://doi.org/10.1021/acs.energyfuels.1c02753>

1546 Yang T, Xue Y, Liu X, Zhang Z (2022). Solidification/stabilization and separation/extraction treatments of
1547 environmental hazardous components in electrolytic manganese residue: a review. *Process Saf Environ* 157,
1548 509-526. <https://doi.org/10.1016/j.psep.2021.10.031>

1549 Yu Q, Li S, Li H, Chai X, Bi X, Liu J, Ohnuki T (2019). Synthesis and characterization of Mn-slag based
1550 geopolymer for immobilization of Co. *J Clean Prod* 234, 97-104. <https://doi.org/10.1016/j.jclepro.2019.06.149>

1551 Zhan X, Hu C, Gong J, Xu T, Li J, Yang L, Zhong S (2018). Co-disposal of MSWI fly ash and electrolytic
1552 manganese residue based on geopolymeric system. *Waste Manage* 82, 62-70.
1553 <https://doi.org/10.1016/j.wasman.2018.10.014>

1554 Zhan X, Wang L, Gong J, Wang X, Song X, Xu T (2021). Co-sintering MSWI fly ash with electrolytic
1555 manganese residue and coal fly ash for lightweight ceramisite. *Chemosphere*, 263, 127914.
1556 <https://doi.org/10.1016/j.chemosphere.2020.127914>

1557 Zhan X, Gong J, Deng R, Wu M (2022). Co-stabilization/solidification of heavy metals in municipal solid
1558 waste incineration fly ash and electrolytic manganese residue based on self-bonding characteristics.
1559 *Chemosphere* 307, 135793. <https://doi.org/10.1016/j.chemosphere.2022.135793>

1560 Zhang B, Wei J, Zeng Z, Xu W, Yu Q (2018). Effects of sulfur on the solidification of cadmium during
1561 clinkerization. ACS Sustainable Chem Eng 6(8), 10645-10653.
1562 <https://doi.org/10.1021/acssuschemeng.8b01970>

1563 Zhang D, Xiao D, Yu Q, Chen S, Chen S, Miao M (2017c). Preparation of mesoporous silica from electrolytic
1564 manganese slags by using amino-ended hyperbranched polyamide as template. ACS Sustainable Chem Eng
1565 5(11), 10258-10265. <https://doi.org/10.1021/acssuschemeng.7b02268>

1566 Zhang J, Peng B, Chai L, Wang J, Wan S (2011). Development of electrolytic manganese slag, shale and fly
1567 ash sintered brick. Environ Sc Technol 1,144-147. <https://doi.org/10.3969/j.issn.1003-6504.2011.01.034>

1568 Zhang X, Liu Z, Wu X, Du J, Tao C (2017b). Electric field enhancement in leaching of manganese from low-
1569 grade manganese dioxide ore: Kinetics and mechanism study. J Electroanal Chem 788, 165-174.
1570 <https://doi.org/10.1016/j.jelechem.2017.02.009>

1571 Zhang X, Tan X, Yi Y, Liu W, Li C (2017a). Recovery of manganese ore tailings by high-gradient magnetic
1572 separation and hydrometallurgical method. Jom 69, 2352-2357. <https://doi.org/10.1007/s11837-017-2521-5>

1573 Zhang Y, You Z, Li G, Jiang T (2013). Manganese extraction by sulfur-based reduction roasting-acid leaching
1574 from low-grade manganese oxide ores. Hydrometallurgy 133, 126-132.
1575 <https://doi.org/10.1016/j.hydromet.2013.01.003>

1576 Zhang Y, Liu X, Xu Y, Tang B, Wang Y, Mukiza E (2019). Preparation and characterization of cement treated
1577 road base material utilizing electrolytic manganese residue. J Clean Prod 232, 980-992.
1578 <https://doi.org/10.1016/j.jclepro.2019.05.352>

1579 Zhang Y, Liu X, Xu Y, Tang B, Wang Y (2020). Preparation of road base material by utilizing electrolytic
1580 manganese residue based on Si-Al structure: mechanical properties and Mn²⁺ stabilization/solidification
1581 characterization. J Hazard Mater 390, 122188. <https://doi.org/10.1016/j.jhazmat.2020.122188>

1582 Zheng F, Zhu H, Luo T, Wang H, Hou H (2020). Pure water leaching soluble manganese from electrolytic
1583 manganese residue: Leaching kinetics model analysis and characterization. J Environ Chem Eng 8(4), 103916.
1584 <https://doi.org/10.1016/j.jece.2020.103916>

1585 Zheng F, Xie W, Zhu H, Hou H (2022). Water column leaching recovery manganese and ammonium sulfate
1586 from electrolytic manganese residue: extremely low water consumption toward practical applications. Environ
1587 Sci Pollut Res 29(53), 80323-80335. <https://doi.org/10.1007/s11356-022-21463-9>

1588 Zhou C, Du B, Wang N, Chen Z (2014). Preparation and strength property of autoclaved bricks from
1589 electrolytic manganese residue. J Clean Prod 84, 707-714. <https://doi.org/10.1016/j.jclepro.2014.01.052>

1590 Zhou F, Chen T, Yan C, Liang H, Chen T, Li D, Wang Q (2015). The flotation of low-grade manganese ore
1591 using a novel linoleate hydroxamic acid. Colloid Surface A 466, 1-9.
1592 <https://doi.org/10.1016/j.colsurfa.2014.10.055>